คอมโพสิทจากกราไฟท์และเบนซอกซาซีนสำหรับการประยุกต์ใช้ในการทำแผ่นไบโพลาร์ในเซลล์เชื้อเพลิง

นายอนุชา เพ็งดำ

วิทยานิพนธ์นี้เป็นส่วนหนึ่งของการศึกษาตามหลักสูตรปริญญาวิศวกรรมศาสตรมหาบัณฑิต
สาขาวิชาวิศวกรรมเคมี ภาควิชาวิศวกรรมเคมี
คณะวิศวกรรมศาสตร์ จุฬาลงกรณ์มหาวิทยาลัย
ปีการศึกษา 2555

GRAPHITE BASED BENZOXAZINE COMPOSITES FOR AN APPLICATION AS BIPOLAR PLATES IN FUEL CELLS

Mr. Anucha Pengdam

A Thesis Submitted in Partial Fulfillment of the Requirements
for the Degree of Master of Engineering Program in Chemical Engineering
Department of Chemical Engineering
Faculty of Engineering Chulalongkorn University
Academic Year 2012

Thesis Title	GRAPHITE BASED BENZOXAZINE COMPOSITES FOR AN APPLICATION AS BIPOLAR PLATES IN FUEL CELLS
By	Mr. Anucha Pengdam
Field of Study	Chemical Engineering
Thesis Advisor	Associate Professor Sarawut Rimdusit, Ph.D.

Accepted by the Faculty of Engineering, Chulalongkorn University in Partial Fulfillment of the Requirements for the Master's Degree

…… Dean of the Faculty of Engineering
(Associate Professor Boonsom Lerdhirunwong, Dr.Ing.)

THESIS COMMITTEE

…….. Chairman
(Professor Suttichai Assabumrungrat, Ph.D.)

……..……. Thesis Advisor
(Associate Professor Sarawut Rimdusit, Ph.D.)

…….. Examiner
(Associate Professor Varong Pavarajarn, Ph.D.)

…….. External Examiner
(Kasinee Hemvichian, Ph.D.)

อนุชา เพ็งดำ : คอมโพสิทจากกราไฟท์และเบนซอกซาซีนสำหรับการประยุกต์ใช้ในการทำแผ่นไบโพลาร์ในเซลล์เชื้อเพลิง (GRAPHITE BASED BENZOXAZINE COMPOSITES FOR AN APPLICATION AS BIPOLAR PLATES IN FUEL CELLS) อ. ที่ปรึกษาวิทยานิพนธ์หลัก : รศ. ดร. ศราวุธ ริมดุสิต, 96 หน้า.

ในงานวิจัยนี้เป็นการการพัฒนาวัสดุที่เหมาะสมและมีประสิทธิภาพเพื่อนำไปประยุกต์ใช้เป็นแผ่นไบโพลาร์ ที่ใช้ในเซลล์เชื้อเพลิงชนิดเยื่อแลกเปลี่ยนโปรตอน (PEMFC) ซึ่งตามหลักการ การนำเอาใช้งานของแผ่นไบโพลาร์แล้ว เราต้องการวัสดุที่มี สมบัติทางความร้อนที่สูง สมบัติทางไฟฟ้าฟ้าที่สูง และมีสมบัติทางกลที่ดี ดังนั้นในงานวิจัยนี้จึงมีวัตถุประสงค์เพื่อศึกษา สมบัติทางความร้อน สมบัติทางไฟฟ้าและสมบัติทางกลของพอลิเมอร์คอมพอสิท ระหว่างพอลิเบนซอกซาซีนซึ่งใช้เป็นตัวเมทริกซ์และใช้สารเติมเป็นกราไฟท์โดยทำการขึ้นรูปภายใต้สภาวะการผสมที่ อุณหภูมิ 200 องศาเซลเซียส ความดันจากเครื่องอัดไฮดลอลิกที่ 15 เมกะปาสคาล เป็นเวลา 3 ชั่วโมง เพื่อให้มั่นใจว่าพอลิเมอร์คอมพอสิทที่เตียมมีการบ่มตัวเต็มที่ องค์ประกอบของกราไฟท์ที่เติมลงไปในคอมพอสิทอยู่ในช่วงระหว่าง 40 ถึง 80 เปอร์เซ็นต์ โดยน้ำหนัก พบว่าค่าความหนาแน่นจะอยู่ในช่วงระหว่าง 1.19-1.88 กรัมต่อลูกบาศก์เซนติเมตร ซึ่งเป็นไปตามทฤษฎี กฎของการผสม จากการทดลองพบว่าปริมาณการเติมกราไฟท์ได้สูงที่สุดอยู่ 80 เปอร์เซ็นต์โดยน้ำหนัก หรือ 68 เปอร์เซ็นโดยปริมาตร พบว่าค่ามอดูลัสการสะสมที่อุณหภูมิห้อง มีค่าสูงถึง 21.9 จิกะปาสคาล ซึ่งมีค่าเพิ่มขึ้นจาก พอลิเบนซอกซาซีนบริสุทธิ์ ที่มีค่า 5.9 จิกะปาสคาล ถึง 370 เปอร์เซนต์ พบว่าอุณหภูมิการเปลี่ยนสถานะคล้ายแก้ว (T_g) ของคอมพอสิทอยู่ในช่วงระหว่าง 174 ถึง 194 องศาเซลเซียส ซึ่งค่าเพิ่มขึ้นตามปริมาณกราไฟท์ที่เพิ่มสูงขึ้นทั้งนี้เกิดจากการที่ ปริมาณความสามารถในการยึดเหนี่ยวที่ผิวของกราไฟท์และเบนซิกซาซีนเพิ่มสูงมากขึ้น พบว่าคอมพอสิทมีความสามารถในการนำความร้อนสูงถึง 10.2 วัตต์ต่อเมตรเคลวิล ที่ปริมาณการเติมกราไฟท์สูงสุด นอกจากนั้นยังพบว่าค่า มอดูลัสของการโค้งงอและ ค่าการทนต่อแรงดัดโค้ง อยู่ที่ 17 และ 52 จิกะปาสคาล ตามลำดับ ค่าการดูดซึมของน้ำมีค่าค่อนข้างต่ำโดยมีค่าประมาณ 0.032 เปอร์เซ็นต์ ที่เวลาผ่านไป 24 ชั่วโมง นอกจากนี้ยังมีค่าความสามารถในการนำไฟฟ้า สูงถึง 245 ซีเมนต์ต่อเซนติเมตร ดังนั้นจากข้อมูล สมบัติทางความร้อน สมบัติทางไฟฟ้า และสมบัติทางกล มีค่าเป็นไปตามความต้องการของ กรมพลังงานของสหรัฐอเมริกา (DOE) จึงทำให้คอมพอสิทระหว่างพอลิเบนซอกซาซีนกับกราไฟท์มีความเหมาะสมเป็นอย่างมากที่จะนำไปประยุกต์ใช้เป็นแผ่นไบโพลาร์ในเซลล์เชื้อเพลิงชนิดเยื่อแลกเปลี่ยนโปรตอน

ภาควิชา วิศวกรรมเคมี ลายมือชื่อนิสิต .....

สาขาวิชา วิศวกรรมเคมี ลายมือชื่อ อ.ที่ปรึกษาวิทยานิพนธ์หลัก .....

ปีการศึกษา 2555

5370666121 : MAJOR CHEMICAL ENGINEERING
KEY WORD: POLYMERCOMPOSITE/ GRAPHITE / FUEL CELL / POLYBENZOXAZINE / BIPOLAR PLATE

ANUCHA PENGDAM: GRAPHITE BASED BENZOXAZINE COMPOSITES FOR AN APPLICATION AS BIPOLAR PLATES IN FUEL CELLS.
THESIS ADVISOR: ASST. PROF. SARAWUT RIMDUSIT, Ph.D., 96 PP.

Development of a suitable and efficient bipolar plate material for polymer electrolyte membrane fuel cell (PEMFC) is scientifically and technically important due to the critical demand on higher thermal properties, higher electrical conductivity and better mechanical properties of this material. This research aims to study electrical conductivity and mechanical properties of highly filled graphite composites utilizing polybenzoxazine as a matrix. The condition for the compression molding to produce highly filled graphite-polybenzoxazine composites was at temperature of 200^{o}C, and pressure of 15 MPa in a hydraulic hot-press machine for 3 hours to assure a fully cured specimen. The composition of graphite filler was achieved to be in the range of 40 to 80% by weight. The densities of the obtained composites were found to be in a range of 1.19-1.88 g/cm^{3} as predicted by rule of mixture. The experimental results revealed that at the maximum graphite content of 80wt% or 68vol% filled in the polybenzoxazine, storage modulus at room temperature of the specimen was raised from 5.9 GPa of the neat polybenzoxazine up to about 21.9 GPa in the composites which is about 370% improvement. The glass-transition temperatures (T_g) of the prepared composites were observed to be ranging from 174 to 194^{o}C and the values substantially increased with increasing the graphite contents implying substantial interfacial interaction between the filler and the matrix. Thermal conductivity as high as 10.2 W/mK is achieved for a graphite filled polybenzoxazine at its maximum filler loading. Furthermore, at graphite content of 80wt% in the polybenzoxazine, the composite's flexural modulus and flexural strength were found to be as high as 17 GPa and 52 MPa, respectively. Water absorption of this filled system was relatively low with the value of about 0.032% at 24 hours. Additionally, electrical conductivity was measured to be 245 S cm^{-1}. Consequently, the data on thermal properties, electrical conductivity and mechanical properties of the graphite filled polybenzoxazine composites indicated the values that highly satisfied the United States Department of Energy (DOE) requirements. Therefore, these graphite filled composites based on polybenzoxazine are highly attractive for bipolar plates in PEMFC applications.

Department : Chemical Engineering Student's Signature .....
Field of Study : Chemical Engineering Advisor's Signature .....
Academic Year : 2012

ACKNOWLEDGEMENTS

The author would like to express my sincerest gratitude and deep appreciation to my advisor, Assoc. Prof. Dr. Sarawut Rimdusit, for his kindness, invaluable supervision, guidance, advice, and encouragement throughout the course of this study.

I also gratefully thank Prof. Dr. Suttichai Assabumrungrat, Asst. Prof. Dr Varong Pavarajarn, and Dr. Kasinee Hemvichian for their invaluable comments as a thesis committee.

This research is supported by the Research, Development and Engineering (RD&E) Fund through National Nanotechnology Center (NANOTEC), National Science and Technology Development Agency (NSTDA), Thailand (Project P-12-00292)

The authors would like to thank The Thailand Institute of Nuclear Technology (TINT) for the assistance on thermogravimetric analysis (TGA) and Mektec Manufacturing Corporation (Thailand) Limited for the kind support in the use of laser flash apparatus.

Additionally, I would like to extend my grateful thanks to all members of Polymer Engineering Laboratory of the Department of Chemical Engineering, Faculty of Engineering, Chulalongkorn University, for their assistance, discussion, and friendly encouragement in solving problems. Finally, my deepest regard to my family and parents, who have always been the source of my unconditional love, understanding, and generous encouragement during my studies. Also, every person who deserves thanks for encouragement and support that cannot be listed.

CONTENTS

PAGE

PAGE

PAGE

LIST OF TABLES

TABLE **PAGE**

LIST OF FIGURES

FIGURE **PAGE**

PAGE

PAGE

PAGE

CHAPTER I

INTRODUCTION

1.1 General Introduction

Polymer electrolyte membrane fuel cell (PEMFC) displays the most promising alternative source of energy for a variety of portable electronic devices, stationary and vehicle applications [1]. The PEMFC operates at relatively low temperature (60-100 ^{o}C) and has a high specific power and compactness. To generate useful current and voltage, individual single fuel cells are connected in series to form stack of cells. Where in a bipolar plate is one of the key components of the fuel cells which consumes around 38% of the total costs and may consume up to 80% of the total weight of the fuel cell stacks. Consequently, one of the important challenges in the development of PEMFCs is the reduction in cost as well as weight of the bipolar plate without compromising their performance and efficiency [2]. The bipolar plate's main functions include carrying current away from each fuel cell, distributing gas fuels within the cell and providing support for the Membrane Electrode Assembly (MEA). The Department of Energy proposed a technical target of bipolar plates for the year 2010, in which the main requirements are flexural modulus >10 GPa, flexural strength >25 MPa water absorption <0.3 at 24 hours and electrical conductivity >100 S cm^{-1} [3].

Nowadays, the most commonly used materials for the bipolar plate have been graphite-based polymer composite, because it has excellent chemical stability to survive the fuel cell environment. It also has good electrical conductivity, resulting in the highest electrochemical power output.

Graphite is the most commonly used material for a bipolar plate. It possesses a good electrical conductivity and excellent corrosion resistance with a low density of about 2.2 g cm^{-3}. However, it lacks mechanical strength and has poor ductility. These limit the minimum plate thickness to about 5-6 mm and machining is usually employed to fabricate the flow channels in the bipolar plate. Machining graphite into complex designs usually employed in bipolar plates fabrication is prohibitively

expensive and time-consuming therefore makes it inappropriate for mass production required for the full scale commercialization of fuel cells [4].

Thermosetting resins are highly attractive as a binder resin of graphite filled composite for bipolar plate because of their relatively ease of compounding with the filler comparing with thermoplastics. Benzoxazine resins are a novel kind of thermosetting phenolic resins that can be synthesized from phenol, formaldehyde and amine group. The curing process of a benzoxazine resin into a polybenzoxazine occurs via a ring-opening polymerization by thermal cure without a catalyst or curing agent and does not produce by-products during cure which results in no void in the products. Polybenzoxazines have been reported to possess outstanding properties such as near-zero volumetric shrinkage upon polymerization, ease of processing or compounding due to low melt viscosity before, high glass-transition temperature (T_g), high thermal stability, and low water absorption [5]. Consequently, highly filled and high performance polymer composites from polybenzoxazines have been successfully developed and reported [6, 7]

In this study, we aim to prepare and characterize properties of graphite-filled composites based on polybenzoxazine for bipolar plate application. Some essential properties such as mechanical properties and electrical conductivity of these highly filled composites will be evaluated.

1.2 Objectives

1. To examine the graphite-filled composites based on benzoxazine resin for an application as bipolar plates in fuel cell.
2. To evaluate the effects of graphite contents on electrical, thermal and mechanical properties of composites based on benzoxazine resin.

1.3 Scope of the study

1. Synthesis of benzoxazine resin by solventless technology.
2. Determination of the optimum composition of graphite filled benzoxazine with varied 0-80% by weight of graphite content.
    - Evaluation of the curing condition of the composites in item (2) by Differential Scanning Calorimeter (DSC).
3. Investigation of thermal properties, mechanical properties and morphology of composites in item (2).
    - Density Accessory Kit
    - Dynamic Mechanical Analyzer (DMA)
    - Universal testing machine (flexural mode)
    - Thermal conductivity measuring apparatus
    - Electrical conductivity measurement

1.4 Procedure of the study

1. Reviewing related literature.
2. Preparation of chemicals and equipment for using in this research such as Graphite, Bisphenol-A, Formaldehyde, Aniline etc.
3. Synthesis of benzoxazine resins (BA-a).
4. Preparation of the graphite filled composites based on benzoxazine resin at various weight ratios of graphite and benzoxazine resin i.e. 0:100, 40:60, 50:50, 60:40, 70:30, 75:25,and 80:20.
5. Determine the mechanical, electrical and thermal properties of the graphite filled composites based on benzoxazine resin as follow

   Mechanical properties

   - Density
   - Flexural properties
   - Water absorption

   Thermal properties

   - Glass transition temperature
   - Thermal degradation
   - Thermal conductivity

   Electrical properties

   - Electrical conductivity
6. Analyze and conclude the experimental results.
7. Preparation of the final report.

CHAPTER II

THEORY

2.1 Proton-exchange membrane fuel cell (PEMFC)

Fuel cells are expected to play a major role in the economy of this century and for the foreseeable future. A number of factors provide the incentive for fuel cells to play a role in future energy supplies and for transportations, including climate change, oil dependency and energy security, urban air quality, and growth in distributed power generation [9]. The successful conversion of chemical energy into electrical energy in a primitive fuel cell was first demonstrated over 160 years ago by lawyer and scientist Sir William Grove in 1843 [10]. These early devices, however, had very low current density. General Electric (GE), a more efficient design in the late 1950s for NASA's Gemini and Apollo space missions, and in addition fuel cell system provided electricity and drinking water for the crew. In developing its fuel cell technology, NASA funded more than 200 research contracts that finally brought the technology to a level that was viable for commercial application [11]. The types of fuel cells under active development include hydrogen fuelled ones such as alkaline fuel cell (AFC), polymer-electrolyte-membrane fuel cell (PEMFC) and phosphoric-acid fuel cell (PAFC) [12].

The polymer electrolyte membrane fuel cell (PEMFC) is a good contender for portable applications and automotive propulsion applications because it provides high power density, solid state construction, high chemical-to-electrical energy conversion efficiency, near zero environmental emissions, low temperature operation ($< 100^{o}C$), and fast and easy start-up [13]. Thus, PEMFC is the fuel cell of interest in this thesis. The first development of PEMFC was by GE for the Gemini space project, but after that, the PEMFC development became dormant. The improvement of PEMFC programs was reactivated in the 1980s, by Ballard Power Systems, subsequently recognized as the world leader in fuel cell technology [11]. The company and spin-off company Automotive Fuel Cell Corporation (AFCC) has dominated the developing automotive

market and has started productions of stationary and portable power applications. For example, the largest fleet of hydrogen fuel cell buses in service was in Whistler, BC, Canada for the 2010 Olympic and Paralympic Winter Games. The twenty transit buses, powered by Ballard's FCvelocity-HD6 power module, provide a 62% reduction in greenhouse gas emissions compared to diesel buses [14].There are now more than 40 companies, for instance General Motors, Toyota, and Honda, involved in the growth of the PEMFC technology, especially in the automotive fuel cell market. Siemens and some Japanese companies have particularly focused on portable and residential fuel cell systems, where potentially high-volume markets are expected [8]. Companies such as Plug Power and Hydrogenics have made significant advances in the lift truck and back-up power market with their low pressure PEMFC technology.

2.1.1 The Operation of A PEMFC [11, 12, 15]

The fuel cell is an electrochemical energy device that converts chemical energy, from typically hydrogen, directly into electrical energy. The electrochemical reactions in fuel cells happen simultaneously on both sides of a membrane: the anode and the cathode. The basic PEM fuel cell reactions are shown as follows.

At the anode,

$$\mathbf{H_2} \rightarrow \mathbf{2H^+ + 2e^-} \qquad (\mathbf{2.1})$$

At the cathode,

$$\frac{1}{2}O_2 + 2H^+ + 2e^- \rightarrow H_2O + 286\ \mathrm{kJ/mol} \qquad (2.2)$$

Overall,

$$H_2 + \frac{1}{2}O_2 \rightarrow H_2O + 286\ \mathrm{kJ/mol} \qquad (2.3)$$

The traditional PEMFC has a polymer electrolyte membrane placed between two gas diffusion electrodes, an anode and a cathode respectively, each usually containing a metal catalyst, such as Pt, supported by an electrically conductive material. The gas diffusion electrodes are exposed to the respective reactant gases: the reduction gas (hydrogen) and the oxidant gas (oxygen/air). An electrochemical reaction occurs at each of the two junctions (three phase boundaries) where one of the electrodes, the electrolyte polymer membrane and the reactant gas interface. Figure 2.1shows a schematic of a PEMFC.

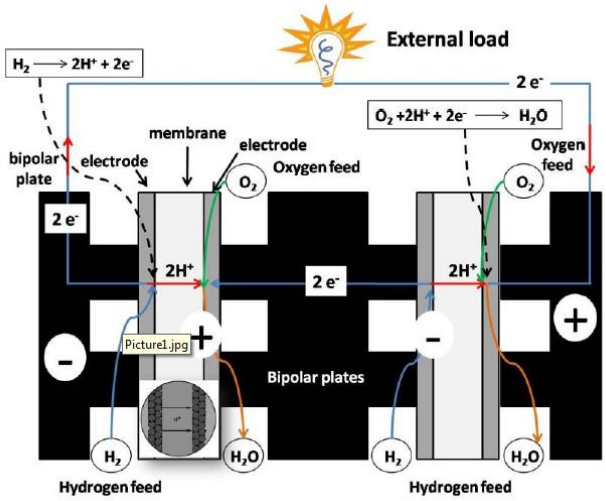

Figure 2.1 Schematic of Polymer Electrolyte Membrane Fuel Cell [11]

During PEMFC operations, hydrogen permeates through the anode and interacts with the noble metal catalyst, producing electrons and protons (Eq. 2.1). The electrons are conducted via an electrically conductive material through an external circuit to the cathode, while the protons are simultaneously transferred via an ionic route through a polymer electrolyte membrane to the cathode. This polymer membrane also serves as a gas barrier so that the reactant species cannot freely combine. At the cathode, oxygen permeates to the catalyst sites where it reacts with the protons and electrons when properly hydrated, producing the reaction (Eq. 2.2). Consequently, the products of the PEMFC reactions are water, electricity and heat. In the PEMFC, current is conducted

simultaneously through ionic and electronic route. The efficiency of PEMFC is largely dependent on ability to minimize both ionic and electronic resistivity. The quality and functionality of fuel cells and their components can be evaluated in terms of conductivity, mechanical strength, permeability, reliability, durability, and power output. A polarization curve is the important indicator of overall fuel cell performance (Eq. 2.2).

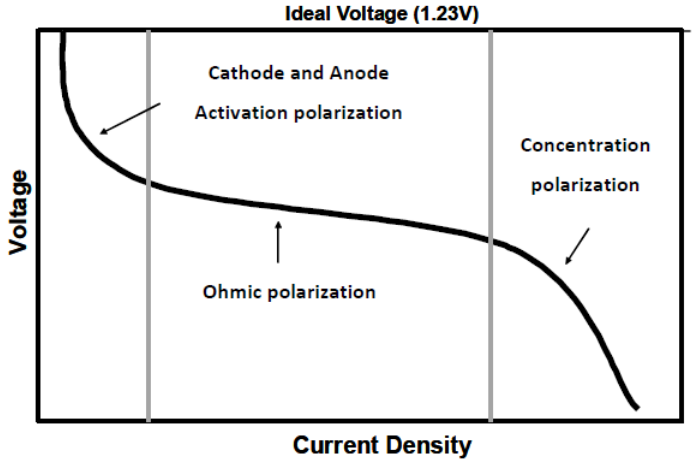

Figure 2.2 Regions of a polarization curve

The plotted curve relates the cell voltage to a changing current density. The maximum cell voltage, which occurs when the current density is zero, is referred to as the open circuit voltage (OCV). In electrochemical systems the voltage decreases as the current density increases and can be divided into three general areas: activation polarization, ohmic polarization, and concentration polarization. As shown in Figure 2.2, at the OCV, no power is produced. The power then increases with increasing current density up to a maximum, the position of which depends on the design and quality of the fuel cell components employed. Beyond the maximum, the drop in cell voltage is stronger than the increase in current density. The overall fuel cell performance is given in Equation (2.4), which signifies the cell voltage as the ideal Nernst voltage (E^o) minus different sources of voltage loss (η).

$$V_{Cell} = E^0 - \eta_{activation} - \eta_{ohmic} - \eta_{concentrat} \quad (2.4)$$

When no current is flowing, the cell voltage should approach the ideal equilibrium potential (E^o). Internal currents will, however, cause losses and lower the open circuit potential below the Nernst potential.

Activation polarization ($\eta_{activation}$) is due to the energy barrier, which must be overcome in order for the electrochemical reaction to occur. The activation energy of an electrochemical reaction is a function of voltage. The oxygen reduction that occurs in the cathode of the PEMFC has relatively slow kinetics, and consequently, the activation energy must be decreased, which results in a particularly large activation polarization. The activation loss is the dominant source of voltage loss at low current densities. The activation loss from the oxygen reduction reaction is related to effective platinum surface area ($A_{Pt,el}$), platinum loading (L_{ca}), current and exchange current density (i_o) as well as the fuel cell current (i) using Equation (2.5) [12].

$$\eta_{activation} = \frac{RT}{n\alpha F} \ln\left[\frac{i}{10\left(L_{ca}\, A_{Pt,et}\right) \times i}\right] \quad (2.5)$$

where T is the absolute temperature, R is the universal gas constant, n is the number of electrons transferred, α is the transfer coefficient (taken to be 0.5), and F is Faraday's constant.

The ohmic loss (η_{ohmic}) is caused by the resistance to conduction of the ionic species through the electrolyte. This loss is a linear function of current density and is proportional to the resistance of the electrolyte, and resistance through electrically conductive components such as the bi-polar plates. The ohmic losses can also be expressed as a function of current using Ohm‟s law as shown in Equation (2.6).

$$\eta_{ohmic} = iR_{\Omega} \tag{2.6}$$

R_{Ω} is the total cell internal resistance, which includes ionic, electronic, and contact resistance. Concentration polarization arises due to a limited supply of reactants at the electrode surface. As the fuel cell is operated at higher currents, the reaction rate at the electrode can become great enough that mass transfer to the electrode cannot replenish all of the reactants that are consumed. Accordingly, the concentration at the surface of the electrode becomes depleted and a concentration gradient is formed between the surface and the bulk, leading to a further voltage loss. At very high currents, mass transfer to the surface becomes the rate determining step, and the reactant concentration at the surface becomes zero, which is referred to as the limiting current and represents the highest current at which the cell can operate. The value of limiting current for a cell is an important parameter for evaluating mass transfer effects. The relationship between concentrations and the concentration polarization is given by Equation 2.7.

$$\eta_{concentrat} = \frac{RT}{nF} \ln\left[\frac{C_B}{C_S}\right] \tag{2.7}$$

C_B is the bulk concentration of reactant (mol.cm^{-3}), and C_S is the concentration of reactant at the surface of the catalyst (mol.cm^{-3}).

2.1.2 PEMFC Components

An expanded view of PEMFC components is shown in Figure 2.1 above. Key components include the membrane-electrode assembly (MEA), bipolar plates (flow field or separator), and seals.

The components of MEA include:

- An electrolyte membrane separates the reduction and oxidation half reactions, and provides an electrical and gas barrier. It allows the protons to pass through to complete the overall reaction while forcing the electrons to pass through an external circuit.
- Anode and cathode dispersed catalyst layers forming the electrodes are the sites for each half cell's electrochemical reaction.
- Two Gas Diffusion Layers (GDL) further improve the efficiency of the system by allowing direct and uniform mass transfer access of the fuel and oxidant to the catalyst layer, and mechanical support to the membrane. In addition to distributing the gases, the anode GDL also conducts the electrons away from the anode. Then the electrons go back to the anode bipolar plate and current collector. The cathode GDL conducts the electrons to the cathode catalyst layer from the cathode bipolar plate and the current collector, ensuring the complete flow of electrons. Typically, porous carbon paper or cloth is the material used for GDLs.
- A solid polymer electrolyte is impregnated with catalyst layers for the anode and cathode. The most common type of electrolyte used in fuel cell applications is a perfluorosulfonic acid (PFSA) polymer, which Dupont supplies under the trade name of Nafion™.

Individual cells are combined into a fuel cell stack of the desired power. End plates and other hardware, such as current collectors, bolts, springs, intake/exhaust pipes, and fittings, are needed to complete the stack. The plates provide an integrated assembly for the entire fuel cell stack. The materials currently available for end plate production should have sufficient mechanical strength; normally steel or aluminum is used. The

current collector typically functions to collect and transfer the current from the stack to an external circuit. A metal material with good electric contact and conductivity, normally copper, is suitable for the collector.

2.2 Bipolar Plates [16]

The bipolar plate performs a number of functions within the PEMFC as described below.

1. Conducting electrons to complete the circuit, including by
    - collecting and transporting electrons from the anode and cathode, as well as,
    - connecting individual fuel cells in series to form a fuel cell stack of the required voltage (i.e., fuel cells are typically arranged in a bipolar configuration);
2. Providing a flow path for gas transport to distribute the gases over the entire electrode area uniformly;
3. Separating oxidant and fuel gases and feeding H_2 to the anode and O_2 to the cathode, while removing product water and un-reacted gases;
4. Providing mechanical strength and rigidity to support the thin membrane and electrodes and clamping forces for the stack assembly;
5. Providing thermal conduction to help regulate fuel cell temperature and removing heat from the electrode to the cooling channels.

The materials of the bipolar plate must have particular properties because of its multiple responsibilities and the challenging environment in which the fuel cell operates. The ideal material should combine the following characteristics (target values below are referenced from the Department of Energy (DOE)) [17]:

1. High electrical conductivity: The electrical conductivity is the most important property for the bipolar plate, especially in the through-plane direction. A target of over 100 S/cm has been set by the DOE.

2. Low contact resistance with the GDL: The contact resistance, which depends on the plate material and thickness, can draw the resistance of the plate itself. Typical values for contact resistance are between 0.1 and 0.2 Ωcm^2.
3. Good thermal conductivity: Efficient removal of heat from the electrodes is imperative for maintaining an even temperature distribution and avoiding hotspots on the membrane. The heat conductivity must exceed $10 Wm^{-1}K^{-1}$ for normal integrated cooling fluids or must exceed 100 $Wm^{-1}K^{-1}$ if heat is to be removed only from the edge of the plate.
4. Thermal stability: The higher-temperature operation places restrictions on certain carbon polymer composites.
5. Gas impermeability: Low gas permeability avoids potentially dangerous and performance-degrading leaks. The gas permeability (specifically of hydrogen, oxygen and nitrogen) must be less than 10^{-4} cm^3/scm^2.
6. High mechanical strength: The bipolar plate is physically forceful and supports the thin components in the cell. The material must have suitable mechanical properties (rigidity, tensile strength, flexural strength) and must not warp. The flexural strength and tensile strength for bipolar plates must be higher than 40 MPa and 41 MPa, respectively.
7. Corrosion resistance: The bipolar plate operates in a warm and humid environment while it is simultaneously exposed to air and fuel over a range of electrical potentials. This situation is ideal for corrosion to occur. The acceptable corrosion is 1.6×10^{-3} mA/cm^2 per 5000hr.
8. Resistance to ion-leaching: If metal ions are released from the plates, they can displace protons in the membrane. The displacement diminishes the ionic conductivity.
9. Thin and lightweight proportions: A fuel cell stack requires many cells to achieve the required power levels for certain applications, so many bipolar plates are needed to accommodate the flow channels and maintain mechanical stability. The maximum weight of a bipolar plate should be 200 g/plate.

10. Low cost and ease of manufacturing: When many bipolar plates are required, their cost should be low to reduce the total price of a fuel cell. The expected cost is $25/kW or < $10/plate.
11. Environmentally benign: Recyclability is a particular concern for fuel cell components.

2.3 Bipolar Plate Development

Challenges facing the commercialization of PEMFCs are large scale manufacturing and materials costs, material durability, material reliability, and hydrogen storage and distribution issues [17]. Currently, efforts to improve the PEMFC cost and reliability for the industry, including the automotive industry, are comprised of reducing the cost and weight of the fuel cell stack, the goal being a 50 kW system of $35/kW and <133 kg in mass [18]. The bipolar plates in the stack require significant improvement, since bipolar plates account for approximately 55% of the PEMFC weight, and 37% of the stack manufacturing and materials cost [19, 20] as shown in Figure 2.3. Accordingly, the development of bipolar plates may present opportunities for cost and weight reductions in PEMFCs.

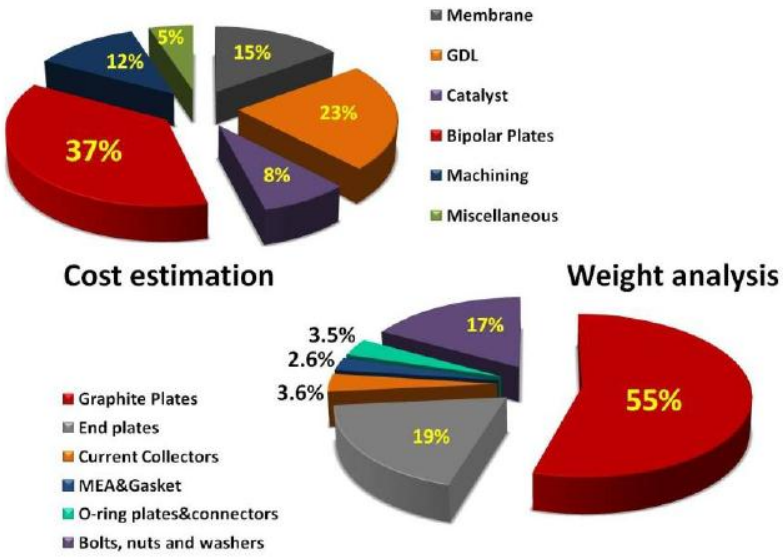

Figure 2.1 Relative cost and weight components from a PEMFC using graphite bipolar plate [19]

Moreover, bipolar plate characteristic requirements are a challenge for any class of materials, and none fits the profile characteristics exactly. Therefore, research on materials, designs and fabrications of bipolar plates for PEMFC applications is a vital issue for scientists and engineers wanting to achieve the appropriate PEMFC for global commercialization. Several types of materials are currently used in bipolar plates, including non-porous graphite plates, metallic plates with or without coating and a number of composite plates.

2.3.1 Non-Porous Graphite Bipolar Plates [16, 21]

Bipolar plates in the PEMFC have traditionally been made from graphite, since graphite has excellent chemical stability to survive the fuel cell environment. Other advantages of graphite are its excellent resistance to corrosion, low bulk resistivity, low specific density, and low electrical contact resistance with electrode backing materials. This low contact resistance results in high electrochemical power output. The disadvantages of graphite plates are its high costs, the difficulty of machining it, its porosity, and its low mechanical strength (brittleness). Bipolar plates have traditionally

been created from graphitic carbon impregnated with a resin or subject to pyrolytic impregnation. A thermal treatment is used in the process to seal the pores. This seal renders the bipolar plates impermeable to fuel and oxygen gases. This type of bipolar plate is available in the fuel cell market from the likes of POCO Graphite and SGL Carbon. Due to the brittle nature of graphite, graphite plates used in fuel cell stacks must typically be several millimetres thick, which add to the volume and weight of the stack.

In order to solve this problem, flexible graphite was considered the material of choice for bipolar plates in PEMFC. Flexible graphite is made from a polymer/graphite composite, in which the polymer acts as a binder. The graphite principally used for the composite is expanded graphite (EG), produced from graphite flakes intercalated with highly concentrated acid. The flakes can be expanded up to a few hundred times their initial volume [22]. The expansion leads to a separation of the graphite sheets into nano-platelets with a very high aspect ratio. This layered structure gives higher electrical and thermal conductivity. The expanded form is then compressed to the desired density and pressed to form the bipolar plate. In comparison to conventional graphite bipolar plates, the bipolar plates produced from EG are thinner.

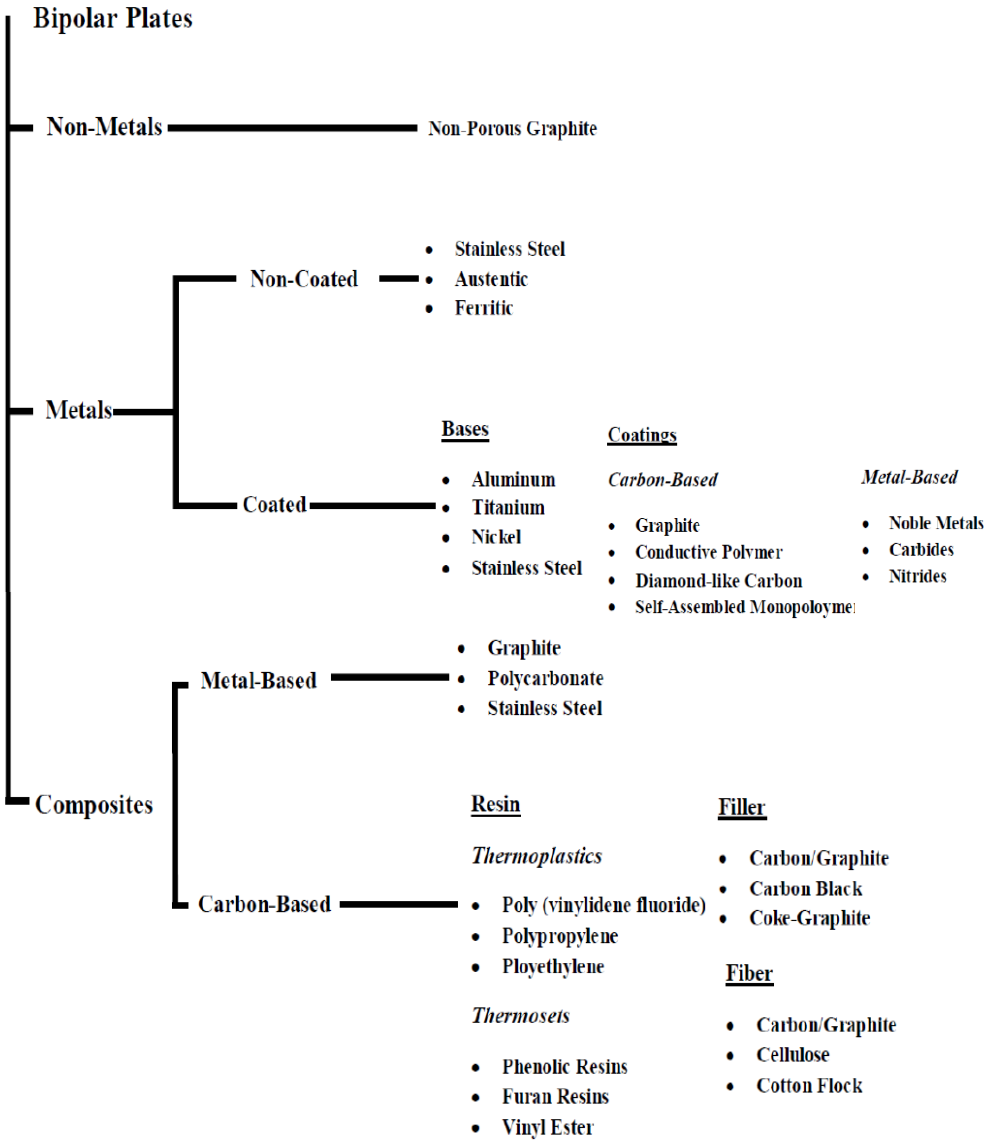

Figure 2.4 Classification of bipolar plate material

Chao Du and his co-operators manufactured a compressed-expanded graphite bipolar plate with a thickness of 1mm [23]. Thinner EG plates, for example the EG/phenol, showed an increase in flexural strength to 40 MPa [24]. However, their compression process for EG composites has not achieved mass production because the production time is too long, and the overall manufacturing cost is high. Manufacturing, for instance, may consist of two steps, pre- and main-curing [24]. In the current market,

flexible graphite bipolar plates are manufactured mainly by GRAFCELL from GraphTech (Ohio, US) for the auto industry.

2.3.2 Metallic Bipolar Plates [16, 21, 25]

Metals, as sheets, are potential candidates for BP material since they have good mechanical stability, electrical and thermal conductivity and gas impermeability. They are also cheaper in the required quantities than graphite plates. Probably the most important benefit is that the resultant stack can be smaller and lighter than graphite bipolar plates. Two advantages to metallic plates that they can be stamped to accommodate flow channels and that the resultant plate can be varied thick, for example 100 μm. However, the main disadvantage of metal plates is their susceptibility to corrosion and dissolution in the fuel cell operating environment of 80^{o}C and a pH of 2.3. This degradation is harmful to fuel cell performance for the following reasons [25]. First, surface oxide creation significantly enlarges the contact resistance between the plate and the GDL. Second, the corrosion process changes the morphology of the surface, potentially reducing the contact area with the GDL. Lastly, when the metal plate is dissolved, the dissolved metal ions diffuse into the PEM membrane and become trapped in the ion exchange sites [27]. This trapping results in ionic conductivity diminution, leading to increased membrane degradation. To solve these issues, researchers have considered of non-coated metal alloys, precious non-coated metals, and coated metals with a protective layer.

Precious Non-coated Metals

Noble metals such as gold and platinum are common material choices, since they perform very similarly to graphite bipolar plates. In some cases, they have shown superior performance [27]. However, the high cost of these metals has prohibited their commercial use.

Non-coated Metals

Aluminum, titanium, and nickel are considered to be possible alternative materials for bipolar plates in PEM fuel cells [25, 29, 30]. The advantages of these metals are their corrosion resistance, low density, low cost, and high strength. Certain higher grades of stainless steel have also been shown to be effective. Some of these materials also have the advantage of being able to diffusion-bond with themselves, allowing complicated flow-field designs to be constructed by overlaying several layers. However, their corrosion resistance results from a passive oxide film that reduces surface conductivity or increases contact resistance. The lower contact resistance causes ohmic losses within a fuel cell. Davies et al. [31] stated that the bipolar plate performance is significantly related to the thickness of the passive layer and surface contact resistance. When the thickness and contact resistance increase, more thermal energy is generated, causing a decrease in output electric energy.

In addition to the contact resistance issues, metallic plates are also quite heavy. Therefore, plates are made as thin as can be out of these materials, allowing for smaller and lighter fuel cells. In the case of nickel, because it does not form a protective oxide layer, it will undergo corrosion in the harsh fuel cell environment. Nickel has to be subjected to surface treatment or alloyed with chromium to make it a feasible choice [25]. Stainless steel alloys are considered to be good candidates for bipolar plate materials because of their low-cost and high strength, and corrosion resistance. Despite this, the environment within fuel cells still proves a challenge for these materials, and corrosion is still a problem for some types of stainless steel such as low-chromium stainless steel [32].

Coated Metals:

To circumvent the disadvantages of metallic bipolar plates, the plates are designed with protective coating layers. The coating material should strongly adhere to the metal substrate and be resistant to cracking, blistering and pinhole formation. Furthermore, to avoid delaminating, the coating layer must have a thermal expansion coefficient similar to that of the underlying metal. Coatings must be conductive and adhere to the base materials to protect the substrate from the operating environment.

Two types of coatings, metal-based and carbon-based, have been investigated. In order to avoid the formation of an oxide layer and nickel dissolution, the SS 316L bipolar plates were coated with a gold layer, having a thickness of less than 2μm [33]. Results clearly demonstrated that there is no difference in the performance of the gold coated bipolar plates and graphite plates; however gold coated plates are relatively more expensive (even if the layer of gold is only nano layers thick). Another possible solution is to coat the metallic bipolar plate with conducting polymer films such as polyaniline (PANI) and polypyrrole (PPy) to protect the bipolar plate while keeping contact resistance low. Shine Joseph and his team electrochemically deposited PANI and PPy on 304SS by cyclic voltammetry with 3 to 15 cycles [33]. Cost, durability and volume production were not mentioned in this study. In another development, conductive polymer coating, a team from INRS-Energie et Matériaux and McGill University in Canada has reported a method of depositing a graphitic protective coating directly onto stainless steel [34]. Current manufacturers of metallic bipolar plates include Nora (Italy) and Dana Corporation (Ohio, US).

2.3.3 Composite Bipolar Plates

Composite bipolar plates are an attractive option for PEMFC use. They not only offer advantages of low cost, lower weight and greater ease of manufacturing than traditional graphite, but their properties can also be tailored through changes of reinforcements and the resin systems. The weakest point of composite bipolar plates is their low electrical conductivity compared to conventional graphite or metallic bipolar plates. To increase the electrical conductivity of the plates, electrically conductive polymers have been used as bipolar plate materials. Electrically conductive polymers are organic based materials that permit electron transfer. There are two types of conductive polymers, which can be explained as follows [35].

1. Extrinsic Conductive Polymers: The combination of conventional polymers (ABS, ABS/PC, and PC & PP) with conductive loads of fillers (e.g. carbon black or carbon fibers, metallic or metallic fibers, metallic powders) allows the creation of new polymeric composite materials with unique electrical properties.

2. Intrinsic Conductive Polymers: These materials are organic polymer semiconductors. Electrical conductivity is realized by the presence of chain unsaturation and electron delocalization effects. Much research effort and interest has therefore been devoted towards the development of polymers with intrinsic electrical conduction characteristics brought about by the presence of the conjugated group and by doping techniques.

In terms of extrinsic conductive polymers, composite materials for bipolar plates can be categorized as metal or carbon-based.

Metal-based Bipolar Plates

Metal-based bipolar plates are made of multiple materials, such as stainless steel, plastic, or porous graphite, so that the benefits of different materials can be harvested in a single bipolar plate. For example, a composite metal-based bipolar plate was fabricated based on porous graphite, polycarbonate plastic and stainless steel [11]. One of the main advantages of porous graphite bipolar plates is the production low cost. However, to produce a plate that is impermeable, the graphite plate is laminated with stainless steel and polycarbonate. The polycarbonate offers chemical resistance and can be molded to provide for gaskets and manifolding. Additionally, stainless steel also contributes rigidity to the structure, while the graphite resists corrosion. The layered plate emerges as a good alternative from reliability and cost perspectives.

Carbon-based Bipolar Plates

Carbon-based bipolar plates can be classified as either carbon-carbon or carbon polymer composites. Carbon-carbon composites are almost entirely made of a carbon matrix reinforced with carbon fibers. The preparation of the composite plate involves an initial slurry-molding process followed by chemical-vapor infiltration (CVI) [18]. During the former process, carbon fibers and phenolic resin were formed into a plaque by means of a vacuum-molding process. After that, the surface of the plaque is sealed by the CVI technique which deposits carbon near the surface of the material, making the plate impermeable to reactant gases and greatly increasing surface electrical conductivity.

Carbon-polymer composites are created by incorporating a carbonaceous material into a polymer binder. The preference for the polymer binder is governed by the chemical compatibility with the fuel-cell environment, mechanical and thermal stability, processability when loaded with conductive filler, and cost. Two different main types of resins are used to fabricate composite plates: thermoplastic and thermosetting. Among the thermosetting resins, such as phenolics, epoxies, polyester, and vinyl ester, etc., the epoxy resin is a popular choice for carbon-polymer bipolar plate production. The thermosetting resins have low viscosity, and thereby contain a higher proportion of conductive fillers. During the molding process, the thermosetting resin allows for molding of intricate details. Moreover, the resins can be highly cross-linked through a proper curing process, and the cross-linked structure gives good chemical resistance.

2.4 Graphite

Graphite is the most crystalline form of carbon, apart from diamond and fullerenes. It exhibits the properties both of metal such as thermal and electrical conductivity and of a non-metal such as inertness, high thermal resistance and lubricity. Usual properties of these fillers are presented in table 2.1. Theses micron fillers present a low specific surface and an aspect ratio close to one and therefore induce little mechanical properties improvement. In addition, their electrical conductivity is rather high compared to others carbon fillers.

Graphite is one of four forms of crystalline carbon; the others are carbon nanotubes, diamonds, and fullerenes. Graphite occurs naturally in metamorphic rocks, such as gneiss, marble, and schist. It is a soft mineral also known by the names black lead, mineral carbon, and plumb ago. The word graphite is derived from the Greek word "graphein" to write [36]. Graphite intercalation compounds are formed by the insertion of atomic or molecular layers of a dierent chemical species called the intercalate between layers in a graphite host material, as shown in Figure 2.5 illustrates the structure of graphite a semi-metallic allotrope of carbon. Graphite features hexagonal ABAB stacking with an interlinear gap that is sufficiently large to permit only Van der Waals interactions between atoms occupying different planes. Very strong covalent bonds exist within each plane, and the exceptionally large cohesive energy of 7.37 eV is primarily responsible for the high melting temperature of graphite. Conductivity is also dependent on crystallographic direction, with a high in-plane conductivity arising from the presence of de-localized electrons. These electrons are further responsible for graphite is dull, metallic appearance and properties of graphite are shown in Figure 2.6 and Table 2.1, respectively [37].

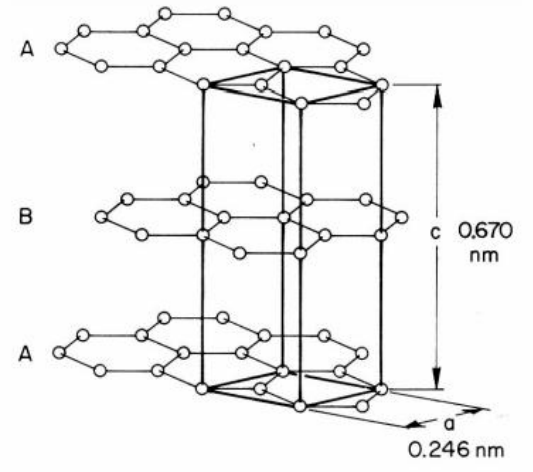

Figure 2.2 The crystal structure of perfect graphite, with the unit cell demarcated in bold lines. Also shown are the characteristic lattice parameters at 0 K [37].

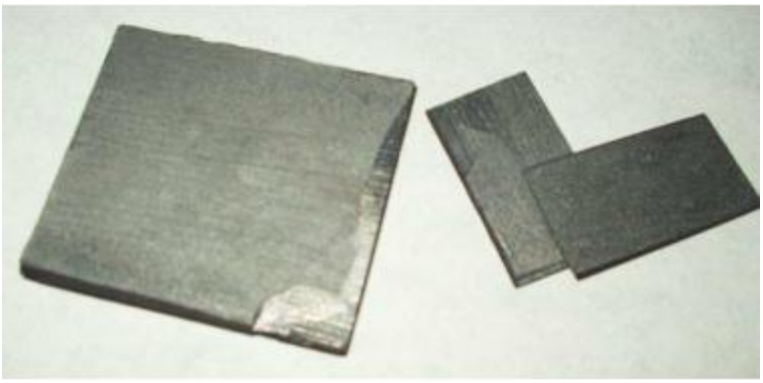

Figure 2.3 Sheets of pyrolytic graphite [37].

Table 2.1 Properties of graphite [38].

Properties	Units	Test	Value
Physical properties			
Chemical Formula	-	-	C
Density, ρ	g/cm^3	ASTM C20	2.25
Color	-	-	black
Crystal Structure	-	-	hexagonal
Water Absorption	%	ASTM C373	0.5 - 3.0
Hardness	Moh's	-	1.0 - 1.5
Mechanical properties			
Compressive Strength	MPa	ASTM C773	96
Tensile Strength	MPa	ACMA Test #4	4.8
Modulus of Elasticity (Young's Mod.)	GPa	ASTM C848	4.8
Flexural Strength (MOR)	MPa	ASTM F417	50
Thermal properties			
Max. Use Temperature	ºC	No load cond.	3650
Thermal Shock Resistance	DT (ºC)	Quenching	200 - 250
Thermal Conductivity	W/mK	ASTM C408	(on plane)
Specific Heat, C_p	cal/gºC	ASTM C351	0.16
Electrical properties			
Electrical Resistivity	Ωcm	ASTM D1829	7×10^{-3}

The unique properties of graphite resulting from its distinctive layered structure and chemical inertness make it the material of choice in many applications:

- Good electrical conductivity: the temperature coefficient of electrical resistance of graphite is negative in a certain range of temperature, unlike that of metals. Near absolute zero, graphite has only a few free electrons and acts as an insulator. As temperature rises, electrical conductivity increases
- Good thermal conductivity: outstanding heat transfer properties
- Unique mechanical strength: the tensile, compressive and flexural strength of graphite increases as temperature increases to 2700 K. At 2700 K graphite has about double the strength it has when at room temperature. Above this temperature its strength falls

- Low coefficient of thermal expansion
- High thermal shock resistance: rapid heating or cooling is not a problem
- Graphite is not wetted by molten glass or by most molten metals
- Low coefficient for friction
- High chemical resistance
- Corrosion resistance: oxidation resistance in air up to 500°C
- Low capture cross-section for neutrons
- Problem-free machining with standard machine tools: graphite can be machined easily. Complicated parts with close tolerances can be machined with precision
- Reasonable cheap material in comparison to other material with similar corrosion resistance
- Graphite does not melt but sublimes at about 3900 K. In air, graphite is resistant to oxidation up to temperatures of about 750 K.
- Graphite displays extremely low creep at room temperature, its flow characteristics being comparable to those of concrete. Creep in graphite is strongly dependent on the grain orientation (creep is defined as plastic flow under constant stress).

Graphite is inert behaviour toward most chemicals and high melting point make it an ideal material for use in: the steel manufacturing process, refractory linings in electric furnaces, containment vessels for carrying molten steel throughout manufacturing plants, and casting ware to create a shaped end-product. In addition, graphite is used as a foundry dressing, which assists in separating a cast object from its mould following the cooling of hot metal. The automotive industry uses graphite extensively in the manufacture of brake linings and shoes. Graphite is an effective lubricant over a wide range of temperatures and can be applied in the form of a dry powder or as a colloidal mixture in water or oil. Other uses include electrodes in batteries, brushes for electric motors, and moderators in nuclear reactors [39].

In this research study, graphite type graphite powder will be selected. Graphite powder with a purity of 95% and a specific density of 2.2 were obtained from the Union Chemical Co., Ltd., Thai. The size of graphite powder is 50 μm.

2.5 Benzoxazine Resin

Benzoxazine resin is a novel kind of phenolic resin that can be synthesized from phenol, formaldehyde and amine. It can be prepared by using solvent synthesis depending on initiator and heating [40]. The resin is developed to provide optimal properties in electronics and high thermal stability applications.

Benzoxazine resin can be classified into monofunctional and bifunctional types depending on a type of phenol used as shown in Figure 2.7 and 2.8, respectively.

Phenol Formaldehyde Aniline Benzoxazine monomer

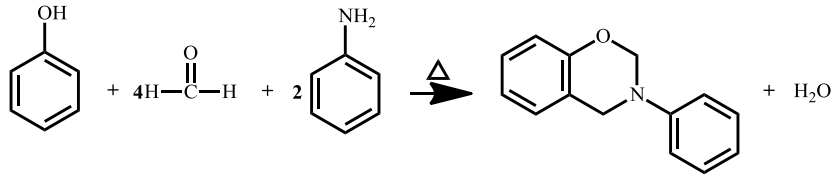

Figure 2.4 Synthesis of monofunctional benzoxazine monomer

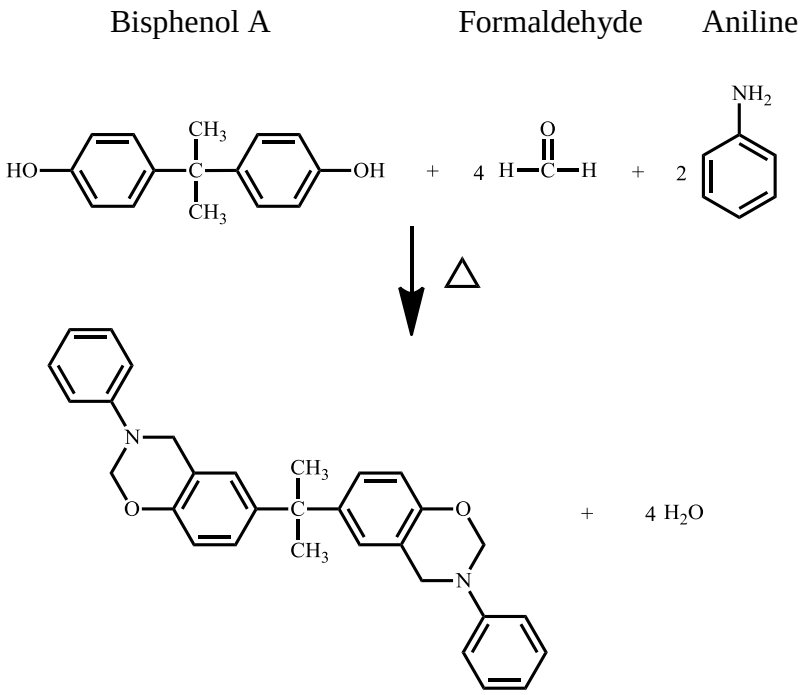

Figure 2.8 Synthesis of bifunctional benzoxazine monomer

Benzoxazine resin can be polymerized by heating and do not need catalyst or curing agent. These two kinds of polybenzoxazine are different in reactant. The benzoxazine monofunction monomer use phenol and the benzoxazine function monomer use bi-phenol to synthesize. Their properties are also different. The benzoxazine bifunctional monomer can be polymerized to yield network structure and the later can be polymerized to yield linear structure. In the binary system, benzoxazine resin with epoxy resin can be polymerized to obtain a high crosslink density and glass transition temperature than polybenzoxazine homopolymer [41, 42].

The polybenzoxazine have excellent thermal, mechanical, electrical, chemical and physical properties such as high moduli, high glass-transition temperature, high char yield, near-zero volumetric shrinkage upon polymerization, low water absorption, low melt viscosity, excellent resistance to chemicals and UV light, and no by-product during cure.

The other advantages of polybenzoxazine include easy processing ability, lack of volatile formation, all attractive for composite material manufacturing. Furthermore, benzoxazine resin is able to be alloyed with several other polymer or resins. In the literature reported that the mixture of the benzoxazine resin with bisphenol-A typed epoxy [41], which the addition of epoxy to the polybenzoxazine network greatly increases the crosslink density of the thermosetting matrix and strongly influences its mechanical properties.

In this research, we use benzoxazine resins which will be synthesized from bisphenol-A, formaldehyde and aromatic amine-based (aniline). Properties and structures of these aromatic amines (arylamines) are shown in Table 2.3 and Figure 2.7, respectively and Figure 2.8 and Table 2.4 show structures and properties of arylamine-based benzoxazine resins.

Table 2.3 Properties of aromatic amines [43]

Properties	Aniline
Molecular weight (g/mol)	93.127
Melting point (°C)	-6.02
Boiling point (°C)	184.17
Density (g/cm^3)	1.0217

Table 2.4 Properties of arylamine-based benzoxazine resin [44]

Properties	BA-a
T_g (DSC)	168
Char yield (% at 800°C)	30
Td at 5% wt. loss (°C)	315
Storage modulus at 28°C (GPa)	1.39
Loss modulus at 28°C (MPa)	15.7
Crosslink density (mol/cm^3)	$1.1x10^{-3}$

CHAPTER III

LITERATURE REVIEWS

Kuan , et al. 2004 [45] investigated the density of the composite bipolar plate increases from 1.49 to 1.82 with increasing graphite content, see Figure 3.1. The density of the composite decreases from 1.70 to 1.45 with the decreasing of graphite size, see Figure 3.2. Increasing the graphite content will reduce the resin content. Since the density of vinyl ester resin (1.03) is much lower than that of graphite (1.88), the density of the composite bipolar plate increases with graphite content. Decreasing the graphite size will increase the voids in the composite bipolar plate. Consequently, density of the plate will be decreased. The density of the plate affects the weight of the fuel-cell stack. The maximum density of the plate for a composite with 80 wt.% graphite is 1.82, i.e., it is lower than that of a pure-graphite bipolar plate, viz. l.88.

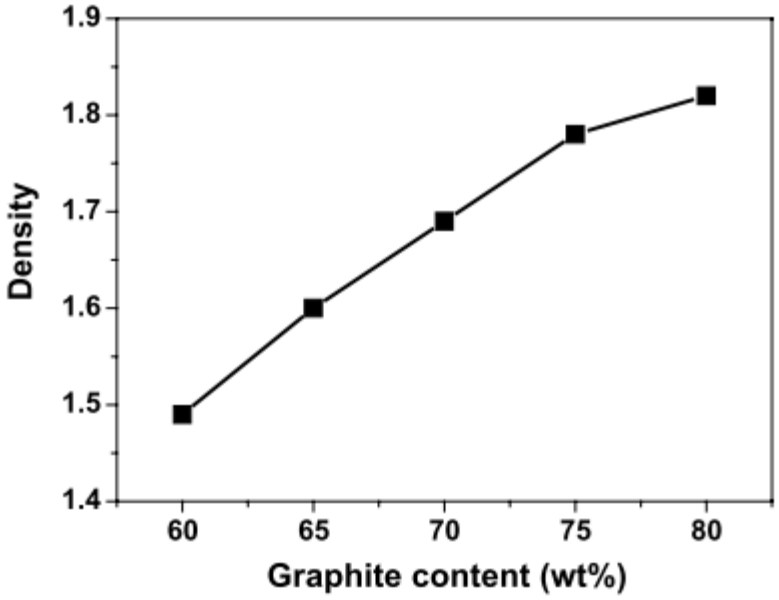

Figure 3.1 Density of composite bipolar plate with different graphite contents.

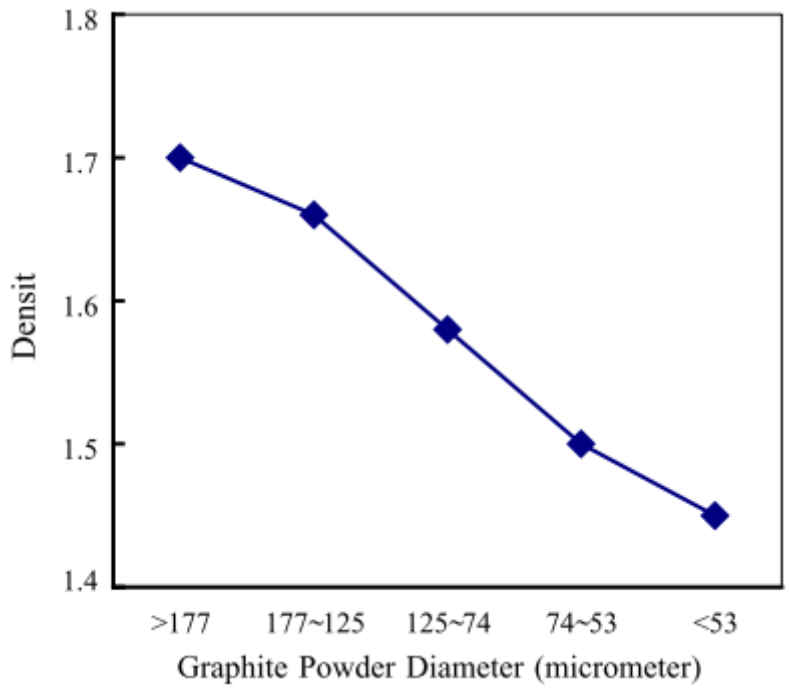

Figure 3.2 Density of composite bipolar plate with 75 wt.% graphite content and with different graphite powder sizes.

Priyanka, et al. 2007 [46] studied the variation in the flexural strength of the carbon paper with decreasing graphite particle size is shown in Figure 3.3a. Initially the strength of the composite increases with decreasing particle size from 46.5 (149-99 µm) to 56.38 MPa (74-49 µm). Decreasing particle size causes aggregation of the particles, which increases the compaction of the plate and results in improved strength. However further reduction in the particle size to less than 37 µm reduces the flexural strength of the plate. This is because reduction in the particle size will increase the number of particles. Small size graphite possesses more surface area than the longer graphite particles. Thus the graphite particles are not completely wetted by the resin. This decreased adhesion between the graphite and resin causes reduction in strength. The variation in the flexural modulus of the composite plate also shows similar behavior (Figure 3.3b) as explained above.

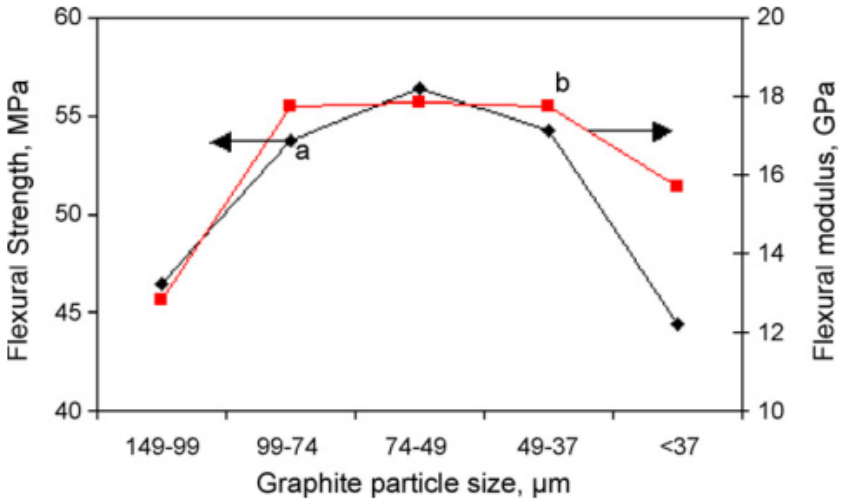

Figure 3.3 Variation in the (a) flexural strength and (b) flexural modulus of the composite plate with decreasing graphite particle size.

Kang, et al. 2010 [47] developed the flexural strengths of composite bipolar plates containing graphite between 60 and 80 wt% filled phenol resin composite are given in Figure 3.4. The flexural strength of the graphite powders having average particle sizes of 75 µm (GR75) composites is higher than that of particle sizes of 150 µm (GR150) counterparts at all loadings of graphite. The data given in Figure 3.4 shows that the flexural strength of the composite bipolar plates decreases with increasing graphite content, which is found with most highly loaded composite systems because the incorporated fillers give a higher probability that cracks are initiated under the load. In addition, post-curing of the composite could increase the strength of the bipolar plates, which is indicated by the dark-grey column in Figure 3.4 in the case of 80 wt% of the GR150 composite system. For this system, the flexural strength of the bipolar composite additionally post-cured at 210 ◦C for 10 min increases from 20.8 to 41.9 MPa. It is believed that post-curing of the composite increases the crosslinking density of the polymer chains and thereby enhances the mechanical strength.

The flexural modulus of composite bipolar plates with graphite loadings between 60 and 80 wt% is presented in Figure 3.5. The flexural modulus of the composite bipolar plates increases with increasing graphite content, and the GR75 composite system shows higher modulus values than the GR150 system. The flexural

modulus of the GR150 composite at 80 wt% is 10.7 GPa, which is raised to 11 GPa after post-curing at 210 ◦C for 10 min, see dark-grey column in Figure 3.5.

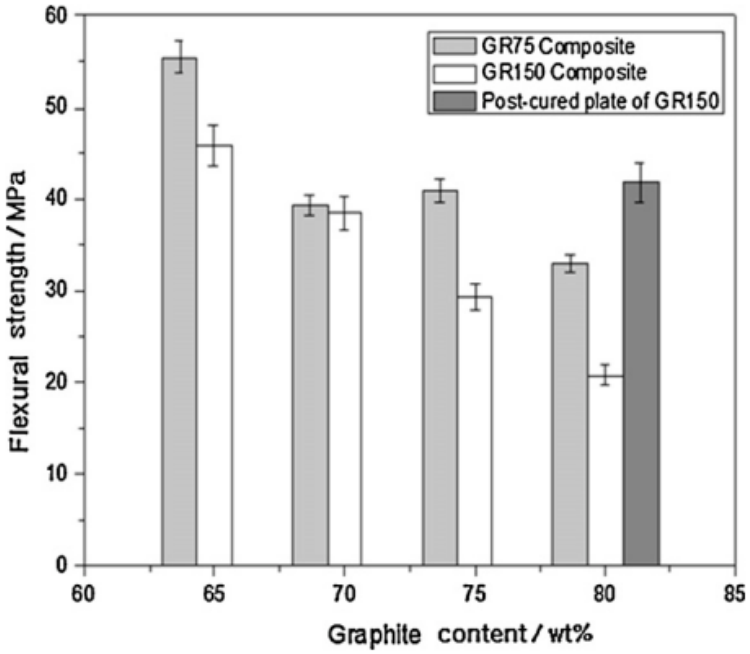

Figure 3.4 Flexural strength of graphite-phenolic resin composites at different graphite contents.

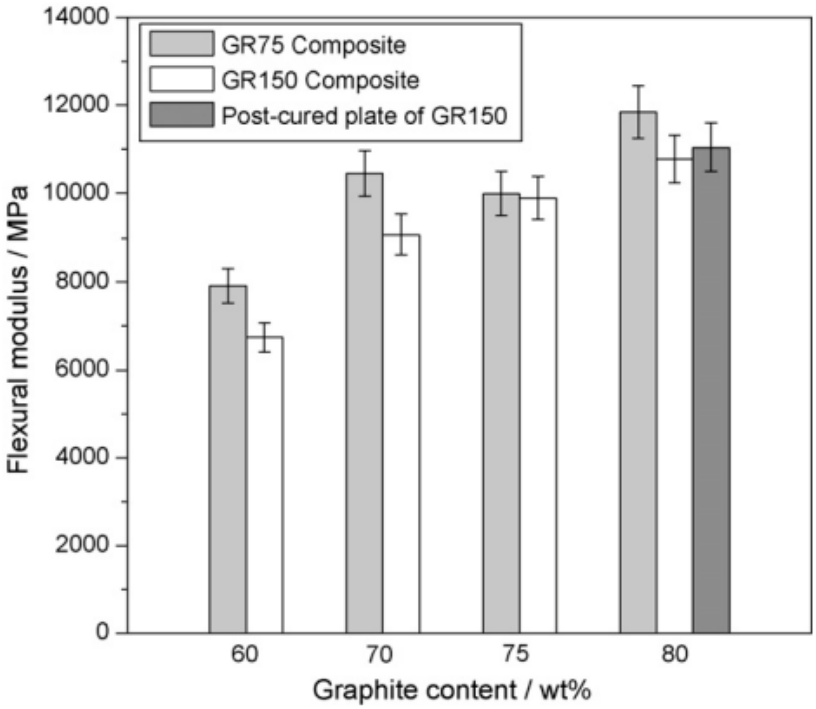

Figure 3.5 Flexural modulus of graphite–phenolic resin composites at different graphite contents.

Chen, et al. 2010 [48] studied bipolar plates must possess good mechanical properties to support thin membranes and electrodes and to withstand high clamping forces for the stack assembly. Flexural strength is an important factor for the bipolar plates of a PEMFC, which should remain unbroken when cell stake was assembled. For example, the target value in literatures indicates the requirement. However, the polymer composites doped with high graphite powder loadings are difficult to reach high conductivity and sufficient mechanical properties at the same time. As a result, the mechanical properties (such as flexural strengths) of composite bipolar plates available so far are still significantly lower than the target values. Two types of resin were used in this study. The results were shown in Figure 3.6.

Figure 3.6 indicates that the flexural strength of the composite plate increases with increasing resin content. As the resin content is increased, the graphite particles can be well wetted by the resin. Hence, the adhesion between resin and graphite become stronger. Consequently, the flexural strength of composite bipolar plate increases. On the other hand, the graphite/novolac epoxy (NE) composite bipolar plate has higher flexural strength due to the more compact three-dimensionally cross linked network structure formed in the curing reaction between NE and phenol formaldehyde resin (PF) as the curing agent. 24 Since the NE has a low shrinkage rate, it reduces the formation of cracks in the finally bipolar plate. It contributes to improving the flexural strength of the plate.

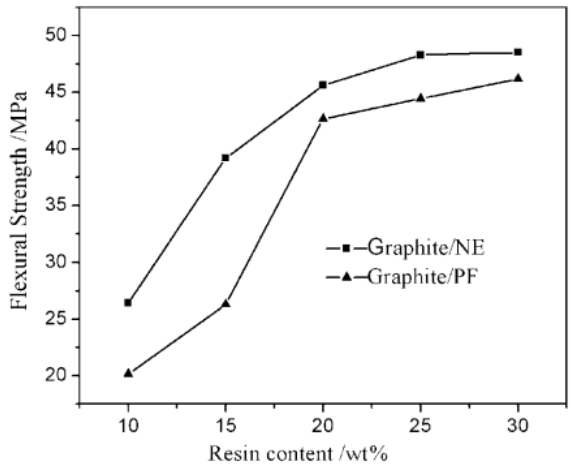

Figure 3.6 Variation in the flexural strength of the composite bipolar plate with increasing resin content.

Electrical conductivity is one of the most important properties of bipolar plates. It was in fluenced by resin content, filler particle size, molding pressure, and curing temperature. The in fluence of the resin content and resin type was mainly discussed in this section. The electrical conductivity of graphite/NE composite bipolar plates is higher than that of graphite/PF at the same conditions and the variational tendency of the electrical conductivity is the same as shown in Figure 3.7.

The conductivity of composite bipolar plates decreases with increasing resin content as shown in Figure 3.7. The conductivity of the composites results from a conductive network formed by the fillers. When the resin content is low, the composites containing a large quantity of conductive fillers, the graphite particles are connected to neighboring graphite particles and generally form surface-to-surface contacts. So the conductive network in the composites has been formed and the density of the conductive network increases with the increase of conductive fillers, which results in higher conductivity of composite bipolar plate.

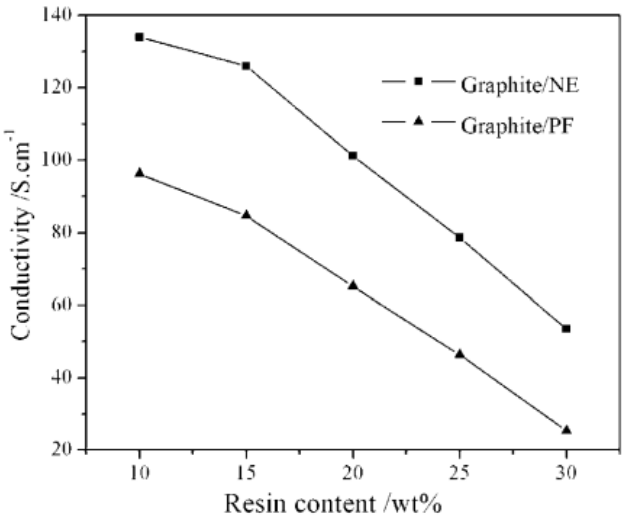

Figure 3.7 Variation in the conductivity of the composite bipolar plate with increasing resin content.

Chen, et al. 2010 [49] studied the effect of graphite particle size on the conductivity was also examined, as shown in Figure 3.8. When the graphite content is below 65 wt.%, the conductivity of 500 mesh graphite powder is slightly higher than that of 300 mesh graphite powder. But when the graphite loading exceeds 65 wt.%, the conductivity of 300 mesh graphite powder becomes significantly higher than that of 500 mesh graphite powder. A reasonable explanation for this phenomenon is that at low concentrations, the 500 mesh graphite powder percolates more easily as compared to the 300 mesh graphite powder due to its small crystal sizes and short distances between adjacent crystals; but when the concentration increases, the 300 mesh graphite powder displays high electrical conductivities because of its low contact resistances.

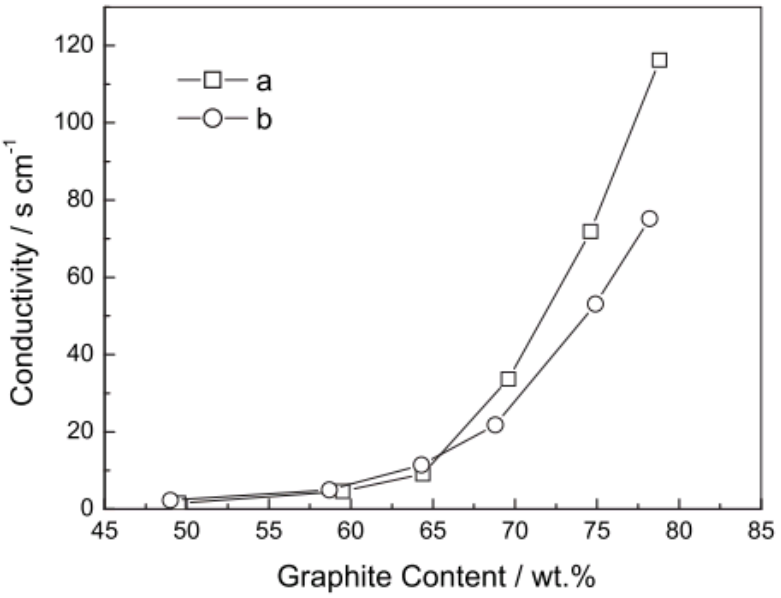

Figure 3.8 In-plane electrical conductivity of polymer–graphite bipolar plates. (a) 300 mesh graphite powder; (b) 500 mesh graphite powder.

Kim, et al. 2010 [50] investigated the Thermo-gravimetric analysis (TGA) curves of prepared graphite powder (GP) and carbon fibre prepreg (CFP) was used for an epoxy (EP) composites are given in Figure 3.9. These curves suggest that the prepared composite has the desired graphite content and a good thermal stability up to 300 ◦C that will be sufficient for application in PEMFCs. There is little improvement in thermal stability with increasing graphite content. The TGA curve of the CFP also shows a similar pattern to that of the composite filled with 70 vol.% GP.

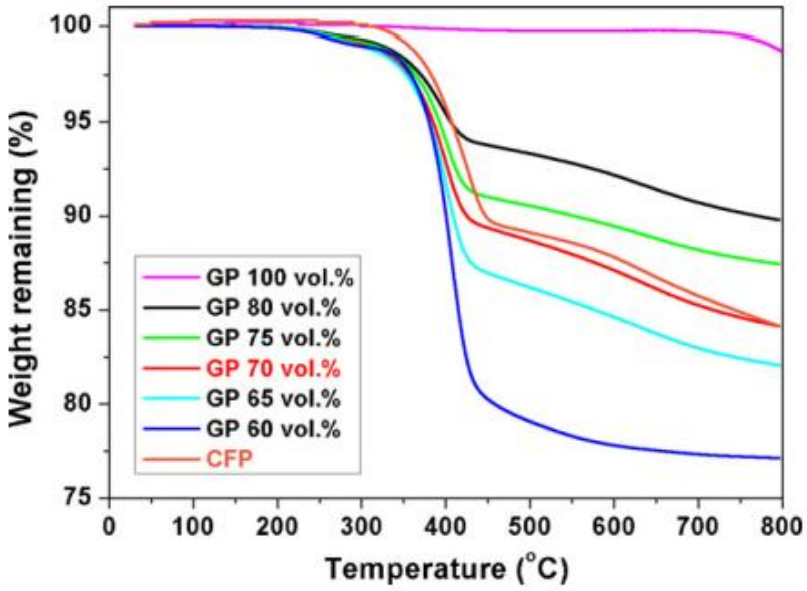

Figure 3.9 TGA curve of GP/EP and CFP composites with various GP contents

Ishida and Rimdusit 1999 [51] studied the lack of the effect of particle size on the specific heat capacity of the composite is again confirmed in Figure 3.10. In this experiment, we mixed two grades of boron nitride which have similar surface area together i.e. HCJ48 with average particle size of 225 µm and TS1890 with average particle size of 75 µm. The composition of the boron nitride in the composites was fixed at 75% by mass. From the figure, as we varied the composition of the large particle grade, we also observed insignificant change in the specific heat capacities of the composites. This confirmed the structure insensitive property behavior of the specific heat capacity of the composite as it is independent on the degree of filler network formation due to the particle size variation. In contrast to the thermal conductivity of this filler-matrix system, we observed a considerable dependence of the composite thermal conductivity on the variation of particle size of the filler [11].

Figure 3.11 shows the effect of filler loading on the specific heat capacities at room temperature of boron nitride-filled polybenzoxazine. Due to the structure-insensitive characteristic of composite specific heat capacity, the effect of filler loading on the composite heat capacity should be predicted by the rule of mixture as expressed in the equation below.

For a two-phase system,

$$C_{pc} = C_{pf}w_f + C_{pp}(1 - w_f) \quad (3.1)$$

C_{pc}, C_{pf} and C_{pp} are the specific heat capacities of the composite, filler, and polymer respectively, w_f is the mass fraction of the filler.

Figure 3.11 shows the plot of the composite specific heat capacity as a function of filler loading ranging from 40 to 90% by mass of filler at 25°C. The plot reveals a linear relationship between specific heat capacity and filler loading. By extrapolating the experimental results to 100% by mass filler loading, we obtain the specific heat capacity value of pure boron nitride with the value of 792 J $K^{-1}kg^{-1}$. The value is close to the published value of 780 J $K^{-1}kg^{-1}$ at the same temperature of 25°C. Also, by extrapolating the experimental results to 0% by mass filler to predict the specific heat capacity of the neat polybenzoxazine resin, we obtain a predicted value of 1383 J $K^{-1}kg^{-1}$ which is close to the measured value of 1415 J $K^{-1}kg^{-1}$. The specific heat capacity values of different filler contents from the experimental results are thus in good agreement with those predicted by the rule of mixture, Eq. (3.1), with an error within ±1.0 %.

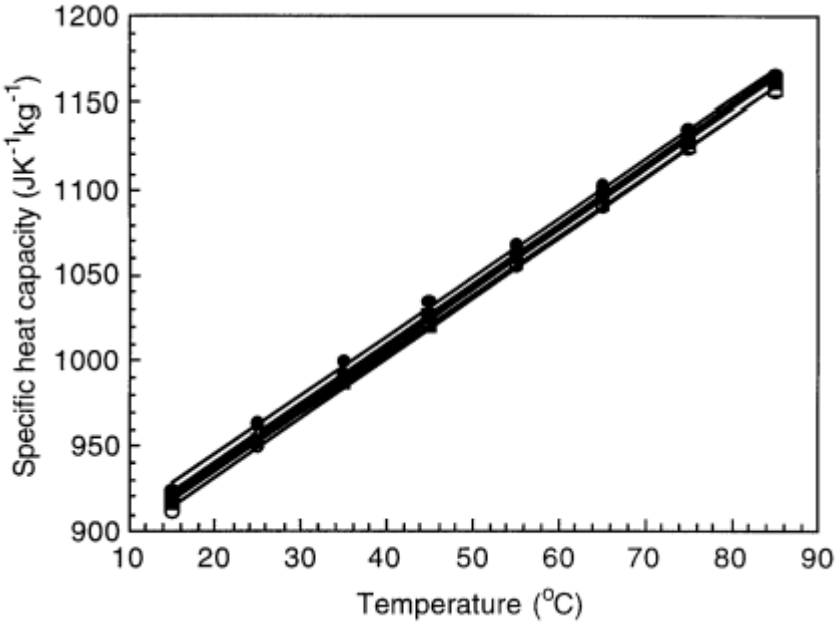

Figure 3.10 Effect of particle size on the specific heat capacity of boron nitride-filled polybenzoxazine. HCJ48:TS1890: ○-100:0, □-80:20, Δ-60-40, ●-40:60, +-20:80, ■-0:100

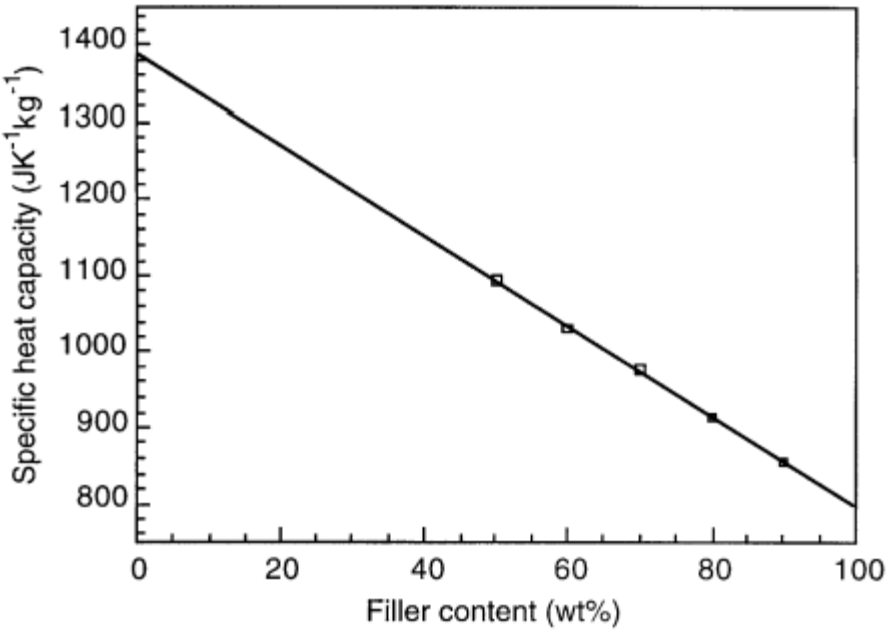

Figure 3.11 Effect of boron nitride contents on the specific heat capacity of its filled polybenzoxazine composites

H. Ishida and S. Rimdusit, 1998 [8] developed highly thermally conductive boron nitride filled polybenzoxazine composites. From Figure 3.12, we can see that, once the conductive networks of the large particle size are formed, the thermal conductivity of the composites will exceed that of the smaller particles as the formation of the conductive paths of the large particles renders less thermal resistance along the paths. The phenomenon is more pronounced at the filler content exceeding the maximum packing of smaller particles since the maximum packing of smaller particle size is less than the maximum packing of the larger particles. Our experimental results are in good agreement with the above statement. We have produced a composite with a remarkably high value of thermal conductivity of 32.5 W/mK at 78.5% by volume of boron nitride filler. The value was averaged from the value of 30.8 W/mK at the center of the sample and 34.2 W/mK at the edge of the sample.

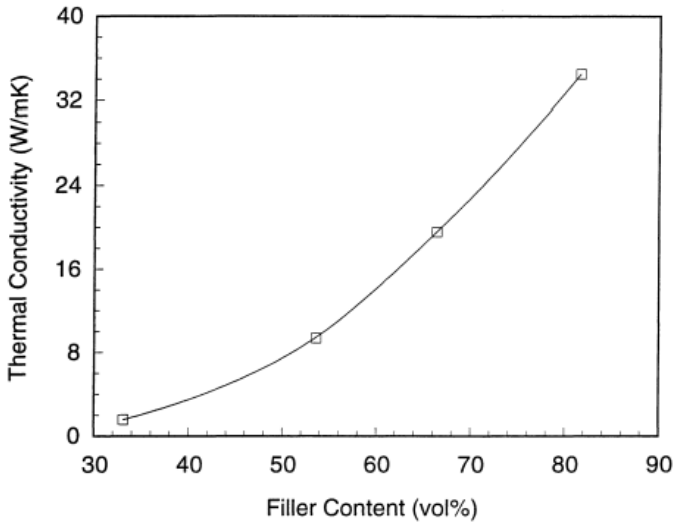

Figure 3.12 Thermal conductivity of boron nitride-filled polybenzoxazine as a function of filler contents.

Xu, et al. 2006 [52] developed the thermal conductivity of Single-walled carbon nanotube (SWNT) reinforced poly(vinylidene fluoride) (PVDF) matrix composites of all volume fractions studied increased with increasing temperature from 25 to 50 oC. The effect of temperature on the thermal conductivity is negligible above 50 oC as shown in Figure 3.13. This is because of the opposing effects of temperature on the specific heat and the thermal diffusivity.

The addition of SWNT decreased the specific heat, as expected from the relatively high specific heat of the polymer matrix. The specific heat was increased with increasing temperature, as expected and as shown in Figure 3.14.

The addition of SWNT increased the thermal diffusivity as expected from the unique SWNT structure which has a much higher thermal diffusivity than that of the polymer matrix. The measured thermal diffusivity of the composites decreased with increasing temperature as shown in Figure 3.15 because the phonon scatterings are enhanced with increasing temperature for polymers.

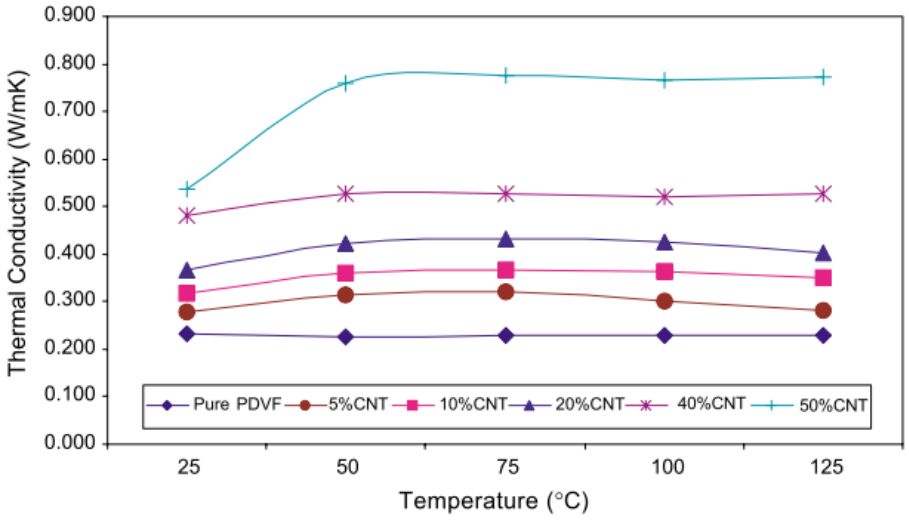

Figure 3. 13 Thermal conductivity of the composites with different volume fractions of SWNTs at different temperature.

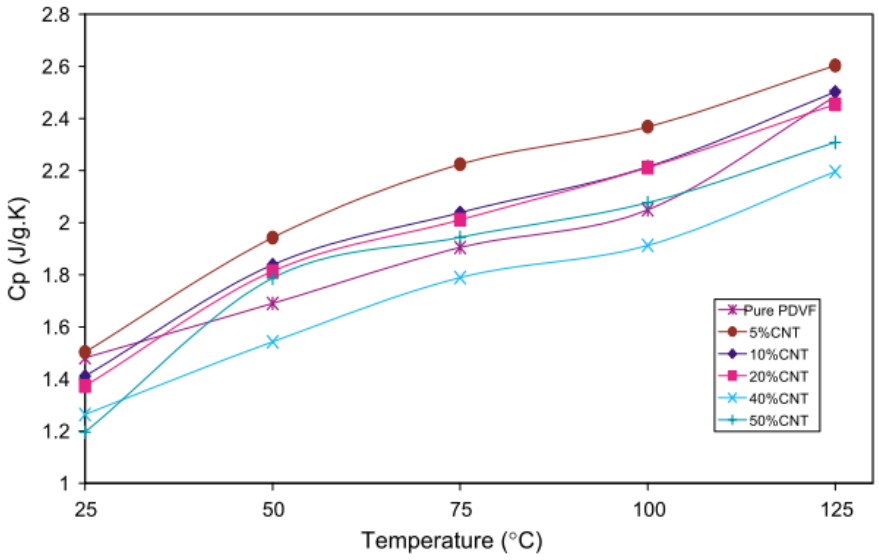

Figure 3. 14 Specific heat of the composites with different volume fractions of SWNTs at different temperature.

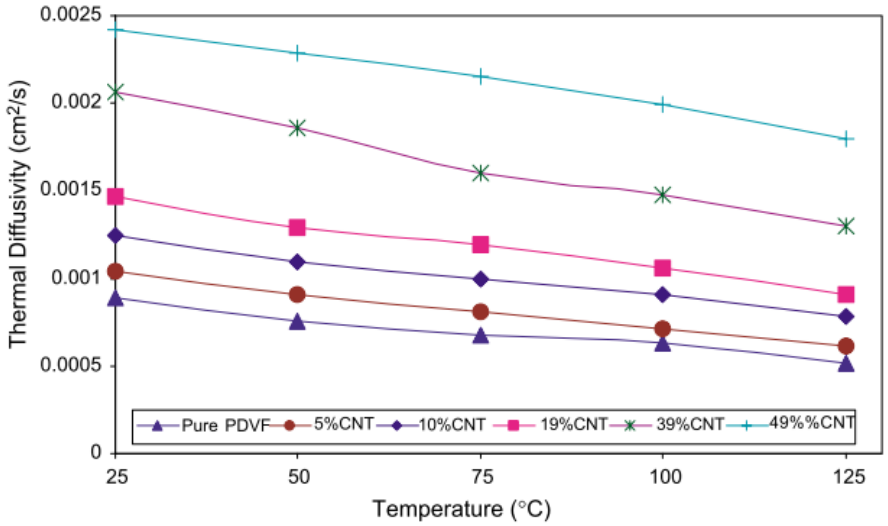

Figure 3.1 Thermal diffusivity of the composites with different volume fractions of SWNTs at different temperature.

Kimura, et al. 2010 [53] studied the morphology of the graphite filled composites was investigated by Scanning electron microscope (SEM). SEM images of fracture surface of the synthetic expanded graphite (BSP-2), filled composites (molded at 200^{o}C for 30 min) based on benzoxazine resin (Ba) and conventional phenolic resin (#200) after flexural test are shown in Figure 3.16. The microstructure of the composite based on benzoxazine resin was quite different from that of the composite based on the conventional phenolic resin. It can be observed that the graphite filled composite based on benzoxazine resin shows even fracture surface, but the graphite filled composite based on the conventional phenolic resin shows uneven fracture surface. It was suggested that the interfacial bond strength between the resin and the graphite of the composite based on the conventional phenolic resin was weaker than that of the composite based on benzoxazine resin. The graphite filled composite based on benzoxazine resin might show better resin distribution and interfacial adhesion between the resin and the graphite.

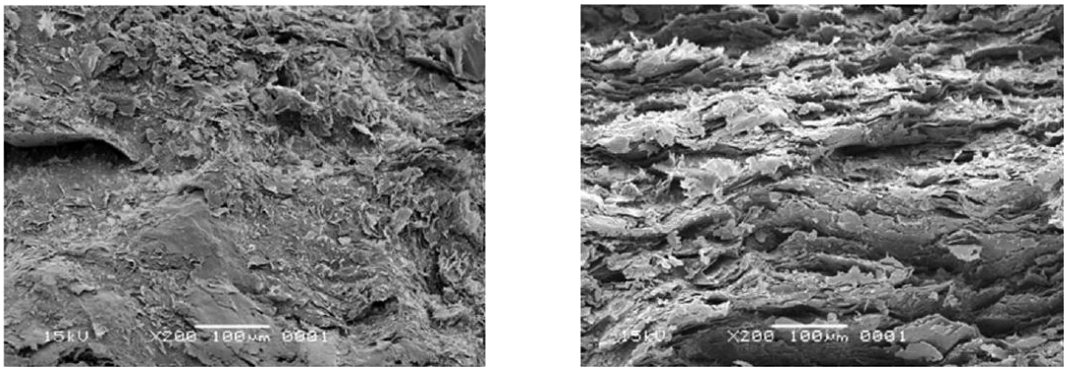

Figure 3.16 SEM micrographs of fracture surface on the expanded graphite (BSP-2) filled composite based on (a) benzoxazine resin, (b) conventional phenolic resin: (#200).

CHAPTER IV

EXPERIMENTAL

4.1 Materials and Monomer Preparation

The materials in this research are benzoxazine resin and graphite. Benzoxazine resin (BA-a) is based on bisphenol-A, aniline, and formaldehyde. Thai Polycarbonate Co., Ltd. (TPCC) supplied the bisphenol-A (polycarbonate grade). Paraformaldehyde (AR grade) was purchased from Merck Company and aniline (AR grade) was obtained from Panreac Quimica SA Company. Graphite powder (size: average 50 μm, purity: 95%) was purchased from Merck Company.

4.1.1 Benzoxazine Monomer Preparation

The benzoxazine resin used is based on bisphenol-A, aniline and formaldehyde in the molar ratio of 1:4:2. This resin was synthesized by using a patented solventless method in the U.S. Patent 5,543,516 (Ishida, 1996). The obtained benzoxazine monomer is clear-yellowish powder at room temperature and can be molten to yield a low viscosity resin at about 70-80 ^{o}C. The product is then ground to fine powder and can be kept in a refrigerator for future-use. The density is 1.2 g/cm^3 and it has a reported dielectric constant of about 3-3.5 (Nair, 2004).

4.1.2 Graphite Characteristics

Graphite powders having average particle sizes of 50 μm were purchased from Merck Corporation. The density is 2.2 g/cm^3 and it has a reported purity of about 95%.

4.2 Specimen Preparation

The graphite filled samples were prepared with graphite loadings of 0, 40, 50, 60, 70, 75 and 80% by weight to yield molding compounds. The graphite was firstly dried at 110^{o}C for 24 hours in an air-circulated oven until a constant weight was achieved and was then kept in a desiccator at room temperature. The filler was mechanically stirred to achieve uniform dispersion in benzoxazine resin using an internal mixer at about 110^{o}C. For thermal-cured specimen, the compound was compression-molded by hot pressing. The thickness was controlled by using a metal spacer. The hot-press temperature of 150^{o}C was applied for 1 hour and 200^{o}C for 3 hours using a hydraulic pressure of 15 MPa. All samples were air-cooled to room temperature in the open mold and were cut into desired shapes before testing.

4.3 Characterization Methods

4.3.1 Differential Scanning Calorimetry (DSC)

The curing characteristic of the benzoxazine-graphite composites were examined by using a differential scanning calorimeter (DSC) model 2910 from TA Instrument. For each test, a small amount of the sample ranging from 5-10 mg was placed on the aluminum pan and sealed hermetically with aluminum lids. The experiment was done using a heating rate of 10^{o}C/min to heat the sealed sample from 30^{o}C up 300^{o}C under N_2 purging. The purge nitrogen gas flow rate was maintained to be constant at 50 ml/min. The processing temperature, time and glass transition temperature were obtained from the thermograms while the percentage of resin conversion was calculated from the DSC thermograms.

4.3.2 Density Measurement

Actual Density Measurement

The density of each specimen was determined by water displacement method according to ASTM D 792 (Method A). All specimens were prepared in a rectangular shape (50 mm × 25 mm × 2 mm). Each specimen was weighed in air and in water at 23±2^{o}C. The density was calculated using Equation (4.1). An average value from at least five specimens was calculated.

$$\rho = \frac{A}{A - B} \times \rho_0 \tag{4.1}$$

where ρ = density of the specimen (g/cm^3)

A = weight of the specimen in air (g)

B = weight of the specimen in liquid (water) at 23 ± 2^{o}C (g)

ρ_o = density of the liquid (water) at the given temperature (g/cm^3)

Theoretical Density Measurement

The theoretical density by mass of polybenzoxazine filled with graphite can be calculated as follow:

$$\rho_c = \frac{1}{\frac{W_f}{\rho_f} - \frac{(1 - W_f)}{\rho_m}} \tag{4.2}$$

Where ρ_c = composite density, g/cm^3

ρ_f = filler density, g/cm^3

ρ_m = matrix density, g/cm^3

ρ_c = composite density, g/cm^3

W_f = filler weight fraction

$(1-W_f)$ = matrix weight fraction

4.3.3 Dynamic Mechanical Analysis (DMA)

The dynamic mechanical analyzer (DMA) model DMA242 from NETZSCH Instrument was used to investigate dynamic mechanical properties. The dimension of specimens was 50 mm × 10 mm × 2.5 mm (W×L×T). The test was performed under the three-point bending mode. A strain in the range of 0 to 30 μm was applied sinusoidally at a frequency of 1 Hz. The temperature was scanned from 30^{o}C to 300 ^{o}C with a heating rate of 5 ^{o}C /min under nitrogen atmosphere. The glass transition temperature was taken as the maximum point on the loss modulus curve in the temperature sweep tests. The storage modulus (G′), loss modulus (G″), and loss tangent (tanδ) were then obtained. The glass transition temperature (T_g) was taken as the maximum point on the loss modulus curve in the DMA thermogram.

4.3.4 Thermogravimetric Analysis (TGA)

A thermogravimetric analyzer model TGA/SDTA 851^{e} from Mettler-Toledo (Thailand) was used to study thermal stability of graphite: polybenzoxazine composites. The initial mass of the composite to be tested was about 10 mg. It was heated from room temperature to 820^{o}C at a heating rate of 20^{o}C/min under nitrogen atmosphere. The degradation temperature at 5% weight loss and solid residue of each specimen determined at 800^{o}C were recorded for each specimen.

4.3.5 Specific Heat Capacity Measurement

Specific heat capacities of all samples were measured using a differential scanning calorimeter (DSC) model 2920 from Perkin-Elmer (Norwalk, CT) Instruments. All samples were crimped in non-hermetic aluminum pans with lids. The mass of the reference and sample pans with lids were measured to within 15-20 mg. The sample was purged with dry nitrogen gas at a flow rate of 60 ml min^{-1}. The test was performed from room temperature up to 200^{o}C at a heating rate of 10^{o}C/min.

4.3.6 Thermal Diffusion Measurement

Thermal diffusivity of the graphite-filled polybenzoxazine composites was measured by laser flash diffusivity instrument (Nano-Flash-Apparatus, LFA 447, NETZSCH). The composite specimens were prepared in a rectangular shape (10 mm×10 mm×1 mm). All measurements were conducted at atmosphere from room temperature to 180^{o}C. In these tests, the specimens were subjected to a short duration thermal pulse by laser. The energy of the pulse absorbed at the front face results in the temperature rise in the rear face. The temperature rise was hem collected by a collecting system. Thermal diffusivity (α) was calculated from the half-rise constant (k= 0.13879 under ideal conditions at half-rise), the specimen thickness (L) and the time ($t_{1/2}$) for the rear face temperature to reach half of its maximum value and thermal diffusion was calculated from Equation 4.3:

$$\alpha = \frac{kL^2}{t_{0.5}} \tag{4.3}$$

For each specimen, its thermal diffusivity was averaged from three measurements at each temperature.

4.3.7 Thermal Conductivity Measurement

The thermal conductivity (k) was calculated using the measured thermal diffusivity (α), specific heat capacity at constant pressure (C_p), and the measured density (ρ) of the sample obtained through Equation 4.4.

$$k = \alpha \times \rho \times C_p \tag{4.4}$$

4.3.8 Flexural Properties Measurement

Flexural properties of the polybenzoxazine composite specimens were determined utilizing a Universal Testing Machine (model 5567) from Instron Instrument. The dimension of the specimens is 50 mm × 25 mm × 2 mm. The test method used is a three-point bending mode with a support span of 32 mm. Bending test was performed at the crosshead speed of 0.85 mm/min. The flexural modulus and the flexural strength of each composite were determined according to the procedure set out in ASTM D 790M, they were calculated by Equations 4.5 and Equations 4.6:

$$E_B = \frac{L^3 m}{4bd^3} \tag{4.5}$$

$$S = \frac{3PL}{4bd^2} \tag{4.6}$$

Where E_B = flexural modulus, MPa

S = flexural strength, MPa

P = load at a given point on the load-deflection curve, N

L = support span, mm

b = width of the beam tested, mm

d = depth of the beam tested, mm

m = slope of the tangent to the initial straight-line portion of the load deflection curve, N/mm.

4.3.9 Water Absorption

Water absorption measurements were conducted following ASTM D570 using disk-shaped specimens having a 50 mm diameter and a 3.0 mm thickness. All specimens were conditioned, weighed, and submerged in distilled water at 25^{o}C. The specimens were occasionally removed, wiped dry, weighed, and immediately returned to the water bath. The amount of water absorbed was calculated based on the initial conditioned mass of each specimen.

4.3.10 Electrical Conductivity Measurement

Electrical conductivity of all samples was measured by a mirror galvanometer with a universal shunt and an HP 4284 impedance analyzer. The HP 4284 programmable current source was used for providing constant voltage drop (V) while current (I) supply in between two pinpoints was measured by HP 4284 auto ranging ampere. The dimension of a round shape specimen was 100 mm in diameter and 2.0 mm in thickness. An average electrical conductivity value from of about 4-5 readings on each plate (in plane) was reported.

4.3.11 Scanning Electron Microscope (SEM)

Interfacial bonding of a filled sample was investigated using an ISM-5400 scanning electron microscope (SEM) at an acceleration voltage of 15 kV. All specimens were coated with thin film of gold using a JEOL ion sputtering device (model JFC-1100E) for 4 min to obtain a thickness of approximately 30Å and the micrographs of the specimen fracture surface were taken. The obtained micrographs were used to qualitatively evaluate the interfacial interaction between the graphite filler and the matrix resin.

CHAPTER V

RESULTS AND DISCUSSION

5.1 Graphite-filled Benzoxazine Resin Characterization

5.1.1 Investigation of Benzoxazine Resin Filled with Graphite Curing Condition

The curing condition of benzoxazine resin filled with high loadings of graphite in a temperature range of 30 to 300^{o}C was performed using differential scanning calorimeter at a heating rate of 10^{o}C/min. Figure 5.1 exhibits the curing exotherms of the neat benzoxazine resin (BA-a) and the benzoxazine-graphite molding compounds at different graphite contents. The thermograms revealed that the onset of curing reaction was at about 150^{o}C. A maximum exothermic peak of all these molding compounds was observed at about 233^{o}C, which is the characteristic of this resin [54]. Such exothermic peak reflects the cure characteristic and suggests appropriate thermal curing scheme of the benzoxazine resin. The unchanged exothermic peak position of the benzoxazine molding compounds implies that graphite has negligible effect on curing reaction of the benzoxazine monomers e.g. curing retardation. However, the area under the curing peaks was found to decrease with increasing the graphite content. This expected phenomenon is related to the decreasing amount of benzoxazine resin in the molding compounds with an increase of the graphite content. Curing retardation has been observed in the systems of cashew nut shell liquid-benzoxazine resin [55], cardanol-benzoxazine resin [56] while curing acceleration was found in epoxy novolac resin-benzoxazine resin [57].

Figure 5.2 presents the DSC thermograms of the benzoxazine molding compound at 40% by weight of the graphite, cured by conventional thermal method. All composites were cured isothermally at 200^{o}C at various times. Determination of the fully cured stage of the compound is shown in Figure 2. A cure temperature of 200^{o}C was used because, at this temperature, polymerization by ring-opening reaction

of the benzoxazine monomer can proceed at a relatively fast rate and provides good cured specimens. From the experiment, the uncured benzoxazine molding compound possesses a heat of reaction determined from the area under the exothermic peak to be 245 J/g and the value decreased to 19, 11 and 4 J/g, after curing at 200^{o}C for 1 hour, 2 hours and 3 hours, respectively. The degree of conversion estimated by Equation (5.1) was calculated to be 98% after curing at 200^{o}C for 3 hours. This curing condition was, thus, used to cure every molding compound to provide the composite samples.

$$\% \text{ conversion} = 1 - \frac{H_{rxn}}{H_0} \times 100 \quad (5.1)$$

Where: H_{rxn} is the heat of reaction of the partially cured specimens.

H_0 is the heat of reaction of the uncured resin.

5.1.2 Actual Density and Theoretical Density Determination of Highly Filled Polybenzoxazine

Figure 5.3 exhibits density of neat polybenzoxazine and graphite filled polybenzoxazine composite at 40, 50, 60, 70, 75 and 80wt% of graphite contents. Density measurements of all composite were used to effectively examine the presence of void in the composite specimens **Error! Reference source not found.**, 58]. This figure shows the theoretical density of the composite bipolar plate in comparison with their actual density. The theoretical density of the composites was calculated from Equation (4.2) whereas the actual density was calculated by Equation (4.1). The calculation is based on the basis that the densities of the graphite and of the polybenzoxazine are 2.22 g/cm^3 and 1.20 g/cm^3, respectively. Due to the higher density of graphite, the results revealed that the theoretical and actual density of the polybenzoxazine composites was increased with the graphite loading following the rule of mixture. The maximum graphite content up to 68% by volume or 80% by weight was achieved in these polybenzoxazine composite. This is due to one outstanding property of polybenzoxazine matrix is its low melt viscosity in which the highly filled void-free composite can easily be obtained. However, the attempt to add graphite higher than 68% by volume was found to provide the experimental density value to be lower than that of the theoretical value due to the presence of void or air

gap in the specimen. Therefore, the maximum graphite loading between the filler and the polybenzoxazine was found to be 68% by volume.

5.1.3 Dynamic Mechanical Analysis (DMA) of Highly Filled Polybenzoxazine

Since all polymers are viscoelastic in nature, dynamic mechanical analysis method is suitable to evaluate complex transition and relaxation phenomena when polymeric materials are presented. Figures 5.4 to 5.6 illustrate dynamic mechanical properties of the graphite filled polybenzoxazine composites with the graphite ranging from 0 to 80wt%. At room temperature, the storage modulus (E') of the graphite filled polybenzoxazine steadily increased with increasing graphite content as seen in Figure 5.4. Furthermore, the modulus of the graphite filled polybenzoxazine in the rubbery plateau region was also found to increase significantly with increasing amount of the graphite. This high reinforcing effect from an addition of rigid particulate filler into the polymer matrix is attributed to the strong interfacial interaction between the graphite and the polybenzoxazine used.

Figure 5.5 exhibits loss modulus (E") curves of the graphite filled polybenzoxazine as a function of temperature. The maximum peak temperature in the loss modulus curve was assigned as a glass transition temperature (T_g) of the specimen. As seen in the inset of this figure, the linear relationship between the glass transition temperature and the filler content was clearly observed. The glass transition temperature of the neat polybenzoxazine was determined to be 174°C whereas the glass transition temperature of the 80% by weight of graphite filled polybenzoxazine is about 194°C. An increase of the T_g with an addition of the graphite is likely due to the good interfacial adhesion between the graphite filler and polybenzoxazine matrix resulting in a high restriction of the mobility of the polymer chains. In addition, Figure 5.6 exhibits α-relaxation peaks of the loss tangent (tanδ) of the graphite filled polybenzoxazine composites. From the figure, it was found that the peak maxima were systematically shifted to higher temperature in good agreement with the loss modulus peak. Tanδ curves obtained from the ratio of energy loss (E") to storage energy (E') in sinusoidal deformation. The magnitude of tanδ peak reflects the large

scale mobility associated with α relaxation, while the width of tanδ relates to the network homogeneity. The peak height of tanδ was found to increase with increasing mass fraction of graphite. This confirmed the reduction in segmental mobility chain with the presence of the hard graphite. These curves become flatter when the graphite content was increased due to the introduction of a rigid segment into the polybenzoxazine matrix as mentioned earlier.

5.1.4 Thermal Degradation of Graphite Filled Polybenzoxazine Composites

Degradation temperature (T_d) is one of the key parameters used to determine temperature stability of polymeric materials. Figure 5.7 exhibits TGA thermograms of the neat polybenzoxazine and graphite filled polybenzoxazine composites at various graphite contents in nitrogen atmosphere. These curves suggest that the prepared composite has the desired graphite content and a good thermal stability at the operating temperature for application in PEMFCs [59, 60]. It was observed that pure graphite exhibits outstandingly high thermal stability with only 0.8% total weight loss up to 800^{o}C. On the other hand, the polybenzoxazine matrix possesses a degradation temperature at its 5% weight loss of 320^{o}C and the char residue at 800^{o}C of 25%. From the thermograms, the degradation temperature at 5% weight loss of the graphite filled polybenzoxazine composites systematically increased with increasing graphite content as seen in the inset of Figure 5.8. The decomposition temperature at the highest graphite content of 80% by weight in the polybenzoxazine was determined to be about 420^{o}C which is about 100^{o}C greater than that of the unfilled polybenzoxazine. This extraordinary enhancement in the thermal properties of the highly filler polybenzoxazine is likely due to the barrier effect of graphite as well as the strong bonding of the benzoxazine resin to the graphite, thus, hence increases the onset degradation of polybenzoxazine [61], which minimize the permeability of volatile degradation products out from the material. The effect of graphite content on the degradation temperature at 5% weight loss of graphite filled polybenzoxazine composites is also summarized in Table 5.1.

The relationship between graphite contents and solid residue of the highly filled polybenzoxazine composites is also reported in Figure 5.8 and the numerical

values listed in Table 5.1. Graphite filler exhibits very high thermal stability thus does not experience negligible weight loss in the temperature range of 30-820^{o}C under the TGA investigation i.e. up to 0.8%. When the temperature is raised to 800^{o}C, only the polybenzoxazine fraction was decomposed thermally and formed char. Therefore, the amounts of solid residue in this case can be approximated to directly correspond to the content of the graphite filler plus char residue of the polybenzoxazine fraction.

The remained solid residue can also be used to quantify the exact amount of the polybenzoxazine in the composite and the calculated amount from their solid residue was also listed in Table 5.1. The calculated amount of the polybenzoxazine was found to be about the same as the amount of the starting benzoxazine resin in the molding compound preparation.

5.1.5 Specific Heat Capacity of Polybenzoxazine and Graphite Filled Polybenzoxazine Composites at Various Graphite Contents

Specific heat capacity (C_p) is a thermodynamic property that describes the ability of a material to store thermal energy. In particular, heat capacity dictates the amount of energy one must put into the system in order to heat the material to a certain temperature [62]. The effect of temperature on composite specific heat capacity at different filler loading is shown in Figure 5.9. From this Figure, an addition of graphite decreased the specific heat capacities systematically, as expected from the lower specific heat capacities of the graphite compared. In this temperature range, the specific heat was found to increase with increasing temperature. The effect of temperature on the specific heat capacities of the composites can be determined from the slope of the plots. From the experimental results, we observed fairly low and stable slopes in our composite systems up to about 140°C. This is due to the high thermal stability and T_g of the polybenzoxazine matrix used. However, within this temperature range, we observed the inflection of the slope of the plot at the temperature about 150°C which is likely due to the glass transitions of these composite materials. The plot reveals a linear relationship between specific heat capacity and filler loading at the temperature below 140^{o}C.

Due to the structure-insensitive characteristic of composite specific heat capacity [51], the effect of filler loading on the composite heat capacity should be predicted by the rule of mixture as expressed in the Equation (5.2).

For a two-phase system,

$$C_{pc} = C_{pf}W_f + C_{pp}(1 - W_f) \quad (5.2)$$

C_{pc}, C_{pf} and C_{pp} are the specific heat capacities of the composite, filler, and polymer respectively, W_f is the mass fraction of the filler.

Figure 5.10 shows the plot of the composite specific heat capacity as a function of filler loading ranging from 40 to 80% by mass of filler at 25°C. We obtain the specific heat capacity value of pure graphite and neat polybenzoxazine with the value of 0.753 and 1.756 $JK^{-1}g^{-1}$, respectively. The values represented in Equation (5.2) will be Equation (5.3).

$$C_{pc} = 0.753W_f + 1.756(1 - W_f) \quad (5.3)$$

The plot reveals a linear relationship between specific heat capacity and filler loading as suggested by Equation (2). The specific heat capacity values of different filler contents from the experimental results are thus in good agreement with those predicted by the rule of mixture with an error within ±1.0 % as seen in Table 5.2. Heat capacity and density are important parameters used to convert thermal diffusivity, a very useful transport property of material.

5.1.6 Effects of Graphite Contents on Thermal Diffusivity of Highly Filled Polybenzoxazine

Thermal diffusivity of graphite filled polybenzoxazine composites as a function of filler content at room temperature is shown in Figure 5.11. As seen in this figure, an addition of highly thermally conductive graphite enhanced the thermal diffusivity of the neat polybenzoxazine significantly, particularly, at high contents of the graphite. At below 50% by weight of graphite, thermal diffusivity of the composites increased slightly with the amount of the filler, however, beyond 50% by weight, the sharp increase in the diffusivity values were clearly observed. This behavior was also observed and reported in the highly filled systems of boron nitride and polybenzoxazine [8], graphite and polystyrene [63], or glass and ethylene vinyl acetate [64]. The behavior was attributed to the formation of tremendous amount of

conductive paths in the filled systems with the loading approaching their maximum packing i.e. highly filled composites. Furthermore, the thermal diffusivities of graphite filled polybenzoxazine as a function of temperature is shown in Figure 5.12. From the figure, it was observed that thermal diffusivity values tended to decrease with increasing temperature as a result of more pronounced phonon-phonon scattering phenomena in the sample [52]. In theory, thermal diffusivity can be converted into thermal conductivity by the relationship expressed in Equation (4.4). In order to determine the thermal conductivities of the composites, densities and heat capacities of the composite are also need.

5.1.7 Thermal Conductivity of Highly Filled Systems of Polybenzoxazine and Graphite

The bipolar plate must be thermally conductive to conduct the generated heat (reaction byproduct) from an active part of the fuel cell to a cooling channel, to control the stack temperature and to achieve a homogeneous temperature distribution in each cell and over the whole active area, therefore; thermal conductivity is a critical bipolar plate characteristic. Table 1 shows the thermal diffusivities, heat capacities, and composite densities of specimens at different compositions and the corresponding values of thermal conductivities determined by Equation (4.4).

Figure 1 show the experimentally measured thermal conductivity of the composites with different graphite weight fractions at 25°C. As it can be seen from the figure, thermal conductivity increases as the filler content increases. When filler concentration reaches 80 % by weight, thermal conductivity increases to 10.2 W/mK, more than 44 times that of pure polybenzoxazine (0.23 W/mK). This rapid growth may be attributed to the significant conductive pathways formed in the composite. As per the recent benchmark given by Department of Energy, USA the recommended value of thermal conductivity for bipolar plate is to be graphite than 10 W/mK [65]. Our highly filled graphite-polybenzoxazine composites at 80% by weight of graphite content are a promising bipolar plate for the fuel cell application as it shows relatively high thermal conductivity. The value is substantially greater than the DOE requirement.

Bond percolation theory gives a phenomenological description of the conductivity of a disordered system near the insulator conductor transition well in path-dependent properties of materials such as electrically conductive composites as a point at which the first conductive path is formed. The filler content, ϕ, at this transition point is called the percolation threshold, ϕ_c. However, thermal conductivity seems to be an intermediate property between a path-dependent property and a bulk property. Hence, the thermal conductivity value in the composite material depends on both the formation of the filler network and the filler loading. Generally, the percolation threshold of thermally conductive composite is difficult to define. In our system, we use a percolation threshold of 0.198 which is the currently accepted percolation threshold for a three dimensional network. Figure 5.14 is the plot between log k and log (ϕ-ϕ_c). The slope of the plot is the critical percolation exponent. From the plot, we obtained the critical exponent having the value of 1.703 which is in good agreement with the theoretical universal value of 2.0 in bond percolation for a three dimensional system [8].

5.1.8 Mechanical Properties of Graphite Filled Polybenzoxazine

In practice bipolar plates require good mechanical properties in order to withstand high clamping forces of the stacking and vibrations during vehicular applications etc. [66, 67]. Flexural modulus and flexural strength of the neat polybenzoxazine and graphite filled polybenzoxazine composites are illustrated as a function of graphite content in Figures 5.15 and Figures 5.16. As seen in Figure 5.15, the modulus values of the composites were found to be substantially improved by the presence of the graphite up to 80% by weight. The flexural modulus of the neat polybenzoxazine was determined to be 5.2 GPa whereas at 40% to 80% by weight of graphite contents, the modulus of the graphite filled polybenzoxazine composites systematically increased from 10.0 to 17.5 GPa. The phenomenon was due to the fact that with substantial interfacial interaction between the filler and the matrix, the addition of more rigid particulate graphite into the polybenzoxazine matrix was able to improve the stiffness of the resulting polymer composites. In addition, it was also found that the modulus of the composites tended to follow an additivity rule. In this work, the flexural modulus of graphite filled composite at 80wt% was found to be

236% higher than that of the neat polybenzoxazine. However, as shown in Figure 5.16, the flexural strength of the graphite filled polybenzoxazine composite bipolar plates was found to decreases with increasing graphite content. It is postulated that the aggregation and agglomeration may present in the graphite thus cause some defects in the composites resulting in lowering of the strength values. These observed phenomena are often observed in graphite-filled systems e.g. graphite-epoxy [68], graphite-phenolic resin [69], graphite-phenol formaldehyde resin and graphite-novolac epoxy [70]. Despite the reduced strength, all the strength data of the polybenzoxazine composites were still much higher than the target value of strength set by DOE i.e. 25 MPa. At maximum graphite loading of 80wt% in polybenzoxazine, its flexural strength is 51.5 MPa which is still much higher than that of graphite-filled epoxy (35 MPa) [68] or graphite-filled phenolic resin (34 MPa) [69] graphite-filled epoxy novalac (45 MPa) [70] etc..

5.1.9 Water Absorption of Polybenzoxazine and Graphite Filled Polybenzoxazine Composites at Various Graphite Contents

The mechanism of water diffusion of the composites was studied from the amount of water absorption by the specimens. The water absorption was calculated from Equation (5.4):

In Equation (5.4), W is the weight of the specimen at time t, and W_d is the weight of the dry specimen [71].

$$\text{Water absorption } (\%) = \frac{W - W_d}{W_d} \times 100 \qquad (5.4)$$

Water absorption for the graphite filled polybenzoxazine composites at different graphite contents are exhibited in Figure 5.17. The percentage of water absorbed plotted against time for all specimens exhibited a similar behavior, i.e., the specimens absorbed water more rapidly during first stages (0-24 hours). The water adsorption values of all graphite/PBA-a composites at different filler contents ranging from 40 to 80% by weight had been recorded up to 168 hours of the immersion i.e. beyond their saturation points. These polybenzoxazine composites show room temperature water uptake having values much less than 0.3% which is the value desired in the industrial standard of typical composites for bipolar plate [72]. The

water uptake of all compositions at 24 hours is <0.11 % and only ca. 0.03% at a filler content of 80% by weight. From the curves, the water uptake up to 168 hours is only 0.2% at the filler content of 40% by weight and lower at higher filler contents, which is considered to be very low. These values were significantly lower than the water absorption values of previous works such as those of graphite filled with epoxy (50wt% Graphite at 24 hours) [73]. Moreover, the water absorption of all samples was also observed to systematically decrease with increasing graphite content. The phenomenon was attributed to the presence of the more hydrophobic nature of the graphite filler in the polymer composites. Good interfacial adhesion as well as excellent wetting of benzoxazine resin with the graphite might also contribute to the substantial reduction of the water absorption values by the addition of the graphite which is highly desirable characteristic in bipolar plate application.

5.1.10 Electrical Conductivity of Graphite Filled Polybenzoxazine

Bipolar plates collect and transport electrons generated by an electrochemical reaction in fuel cell stacks. Therefore, the materials for bipolar plates require high electrical conductivity to minimize voltage loss. In polymer composite, the property is largely influenced by the total filler loading and filler type [74]. The composite filled with graphite has anisotropic electrical conductivity depending on the distribution direction of the fillers. Figure 5.18 shows electrical conductivity of the highly filled systems of graphite and polybenzoxazine composites at different weight fraction of graphite. It is evident that the conductivity of the composite increased non-linearly with an increase in graphite content up to 80% by weight. At 40-60% by weight of the graphite, the electrical conduction values increased only slightly with the filler loading. Beyond 60% by weight of the graphite filler, the conductivity values tended to increase sharply up to about 245 Scm^{-1}. The phenomenon is due to the gradual formation of the percolating network of the graphite particles within the plate with an increase in the graphite content [75]. As per the recent benchmark given by Department of Energy, USA the recommended value of electrical conductivity for bipolar plate is to be graphite than 100 Scm^{-1} [76]. Our highly filled graphite-polybenzoxazine composites at 70 and 80% by weight of graphite content are a promising bipolar plate for the fuel cell application as it shows relatively high

electrical conductivity of 104 and 245 Scm^{-1}, respectively. The value is substantially greater than the DOE requirement.

5.1.11 SEM Characterization of Graphite Filled Composites

Figure 5.19(a) to 5.19(d) shows the interfacial characteristics along the fracture surface at 500 times and 5,000 times magnification of the pure graphite, the neat polybenzoxazine and the graphite filled polybenzoxazine. A SEM micrograph of the graphite platelets is shown in Figure 5.19(a). These platelets are flake-like shaped, and they consist of stacks of thin plates. Figure 5.19(b) show the fracture surface of pure polybenzoxazine to be much smoother when compared to that of the graphite filled polybenzoxazine composite due to the addition of graphite filler are improve the loading area that enhance the polybenzoxazine matrix deformation. Figure 5.19(c) and Figure 5.19(d) shows the SEM micrographs of the graphite filled polybenzoxazine composites with filler content of 5 and 80 % by weight, respectively. The graphite filled composite based on benzoxazine resin relatively shows good graphite distribution and substantial interfacial adhesion between the matrix and the graphite. These results might be attributed to the very low viscosity and good flow-ability of the benzoxazine resin at the molding temperature. When the graphite content is 80 % by weight, the fractured surface exhibits a layered feature because the graphite plates show some alignment in the in-plane direction during the compression molding process with negligible voids. It is, therefore, concluded that that the graphite fillers in the composites are in good contact with each other to give a well-developed electrical pathway and high electrical conductivity at the high graphite loading above.

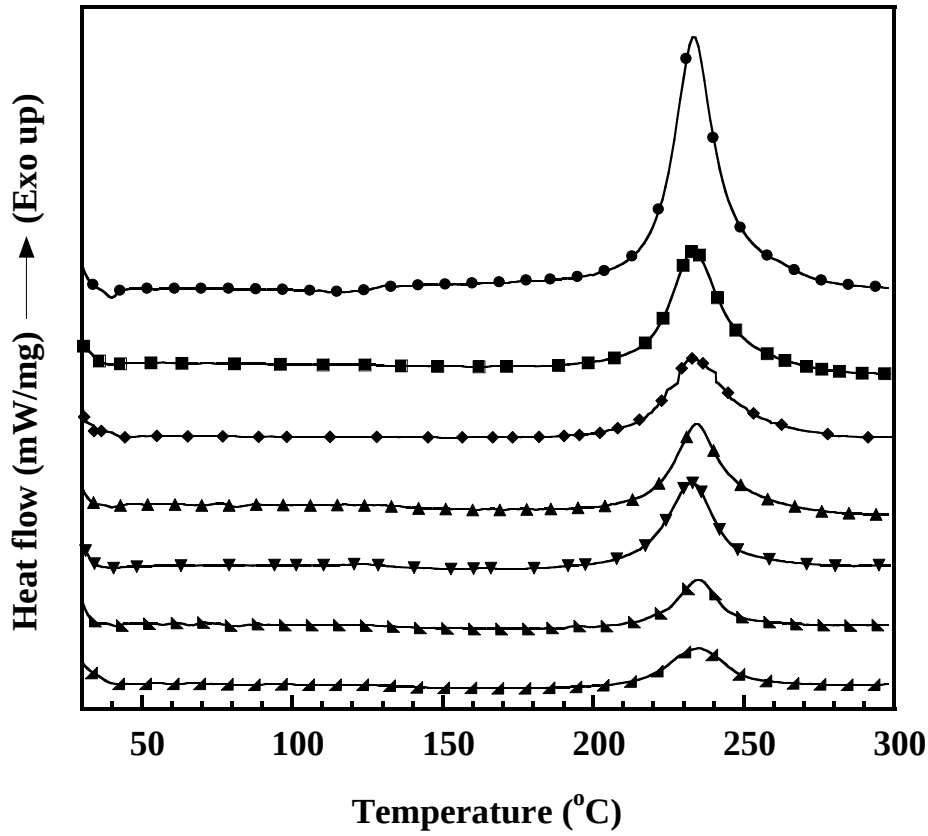

Figure 5.1 DSC thermograms of benzoxazine molding compound at different graphite contents: (●) neat benzoxazine monomer, (■) 40wt%, (♦) 50wt%, (▲) 60wt%, (▼) 70wt%, (◣) 75wt%, (◢) 80wt%.

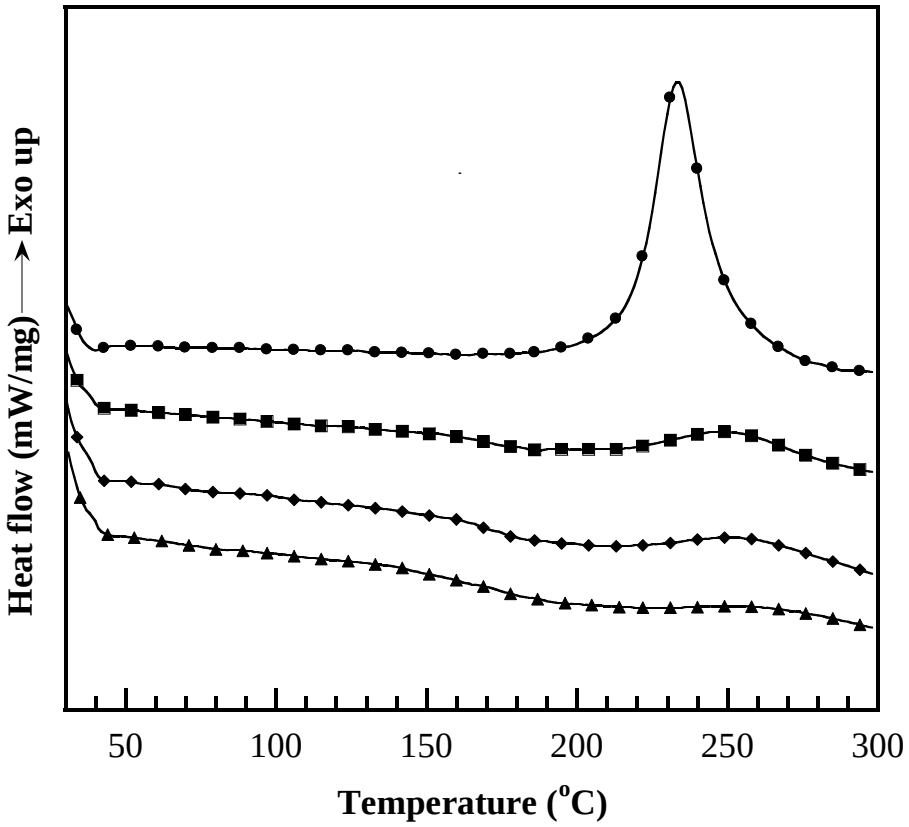

Figure 5.2 DSC thermograms of the composite (40wt% graphite) at various curing times at 200°C: (●) Uncured molding compound, (■) 1 hour, (♦) 2 hour, (▲) 3 hour

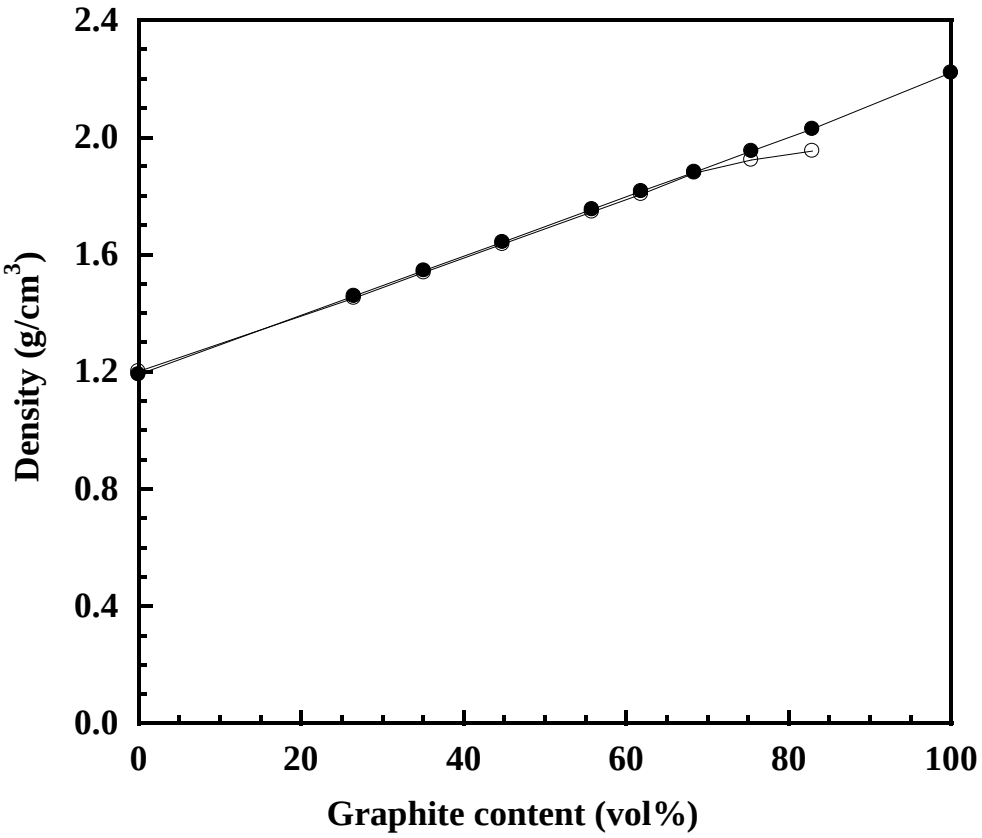

Figure 5.3 Theoretical and actual density of graphite filled polybenzoxazine composites at different content of graphite: (●) theoretical density, (○) actual density.

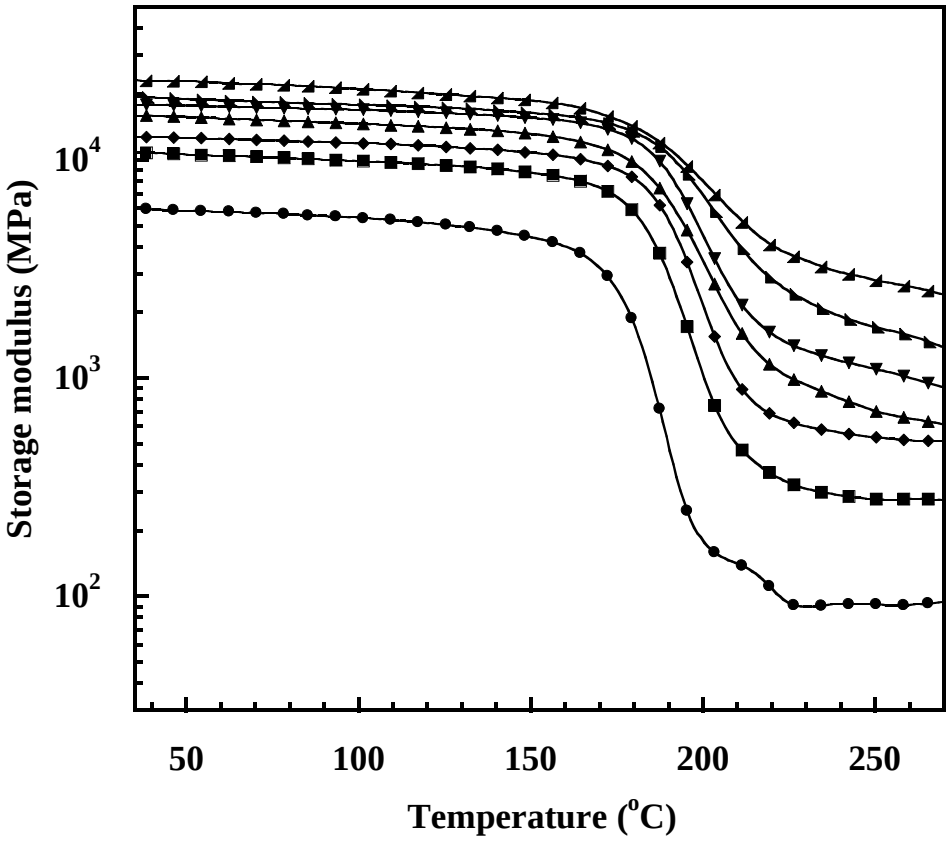

Figure 5.4 DMA thermograms of storage modulus of graphite filled polybenzoxazine composites: (●) neat benzoxazine monomer, (■) 40wt%, (♦) 50wt%, (▲) 60wt%, (▼) 70wt%, (◣) 75wt%, (◢) 80wt%.

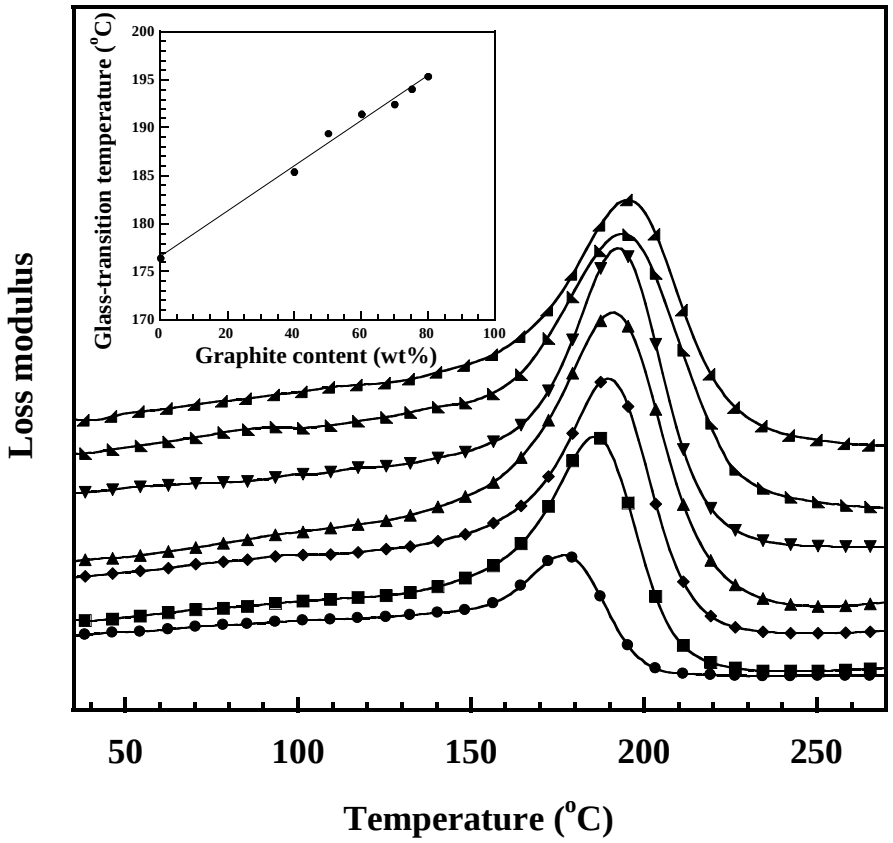

Figure 5.5 DMA thermograms of loss modulus of graphite filled polybenzoxazine composites: (●) neat benzoxazine monomer, (■) 40wt%, (♦) 50wt%, (▲) 60wt%, (▼) 70wt%, (◣) 75wt%, (◢) 80wt%.

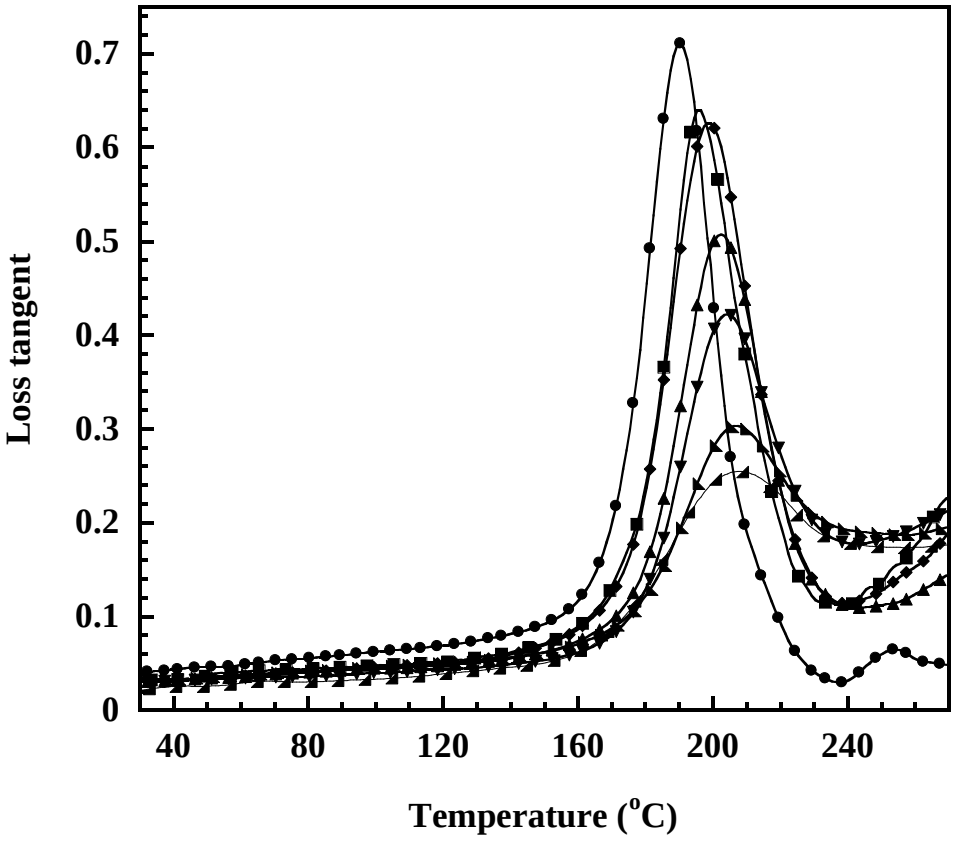

Figure 5.6 DMA thermograms of loss tangent of graphite filled polybenzoxazine composites: (●) neat benzoxazine monomer, (■) 40wt%, (♦) 50wt%, (▲) 60wt%, (▼) 70wt%, (◣) 75wt%, (◢) 80wt%.

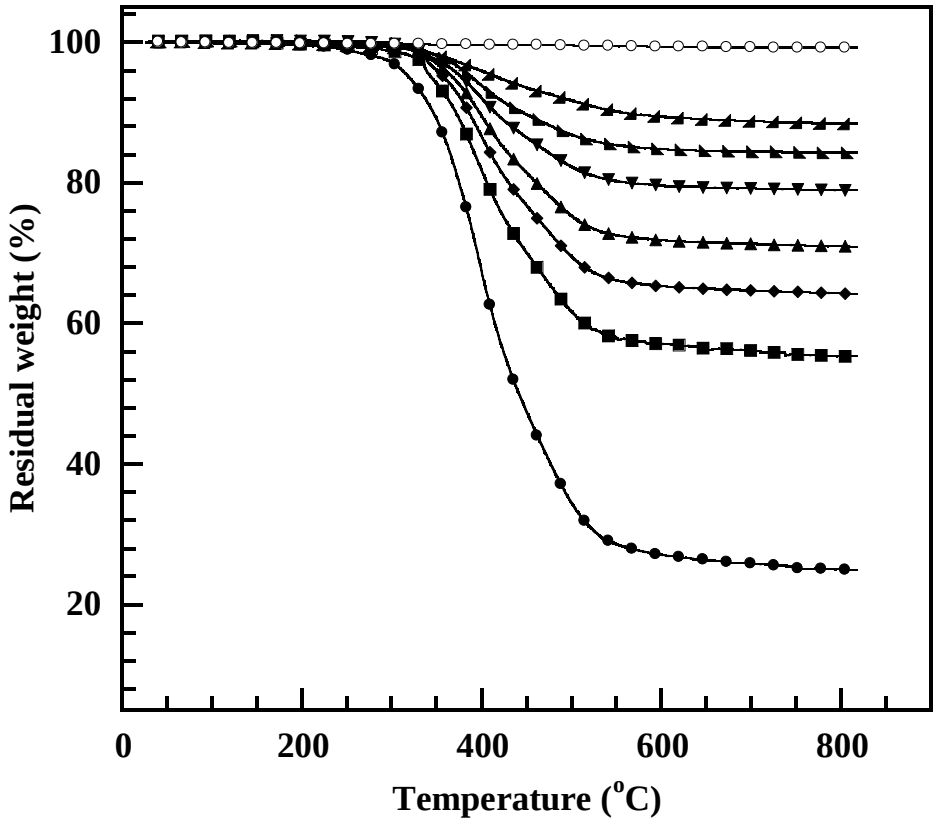

Figure 5.7 TGA thermograms of graphite filled polybenzoxazine composites: (●) neat polybenzoxazine (■) 40wt%, (♦) 50wt%, (▲) 60wt%, (▼) 70wt%, (◣) 75wt%, (◢) 80wt%, (○) neat graphite

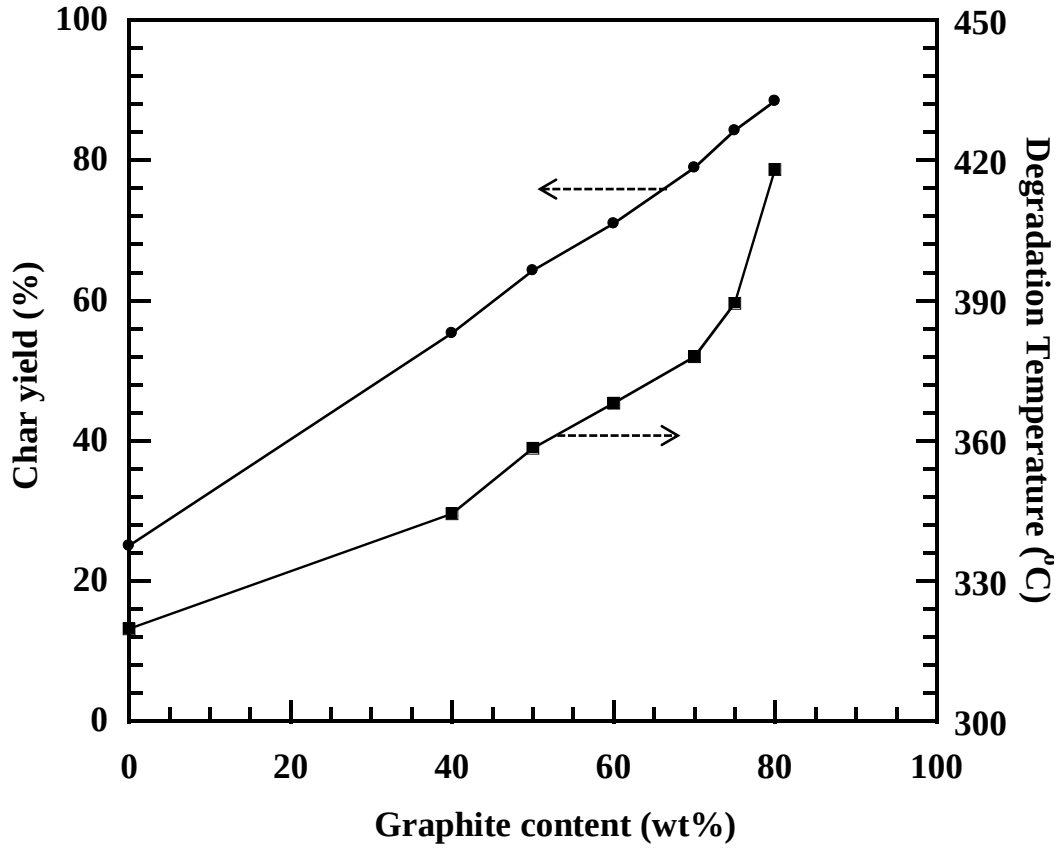

Figure 5.8 (●) Char yield (800°C) and (■) degradation temperature (5%Wight loss) of graphite filled polybenzoxazine composites

Table 5.1 Thermal characteristics of polybenzoxazine and graphite filled polybenzoxazine composites.

Resins	Degradation Temperature (^{o}C) at 5% weight loss	Solid residue (%) at 800^{o}C
PBA-a	320	25.00
40% Graphite/ PBA-a	344	55.32
50% Graphite/ PBA-a	358	64.26
60% Graphite/ PBA-a	368	70.95
70% Graphite/ PBA-a	378	78.91
75% Graphite/ PBA-a	389	84.26
80% Graphite/ PBA-a	418	88.39

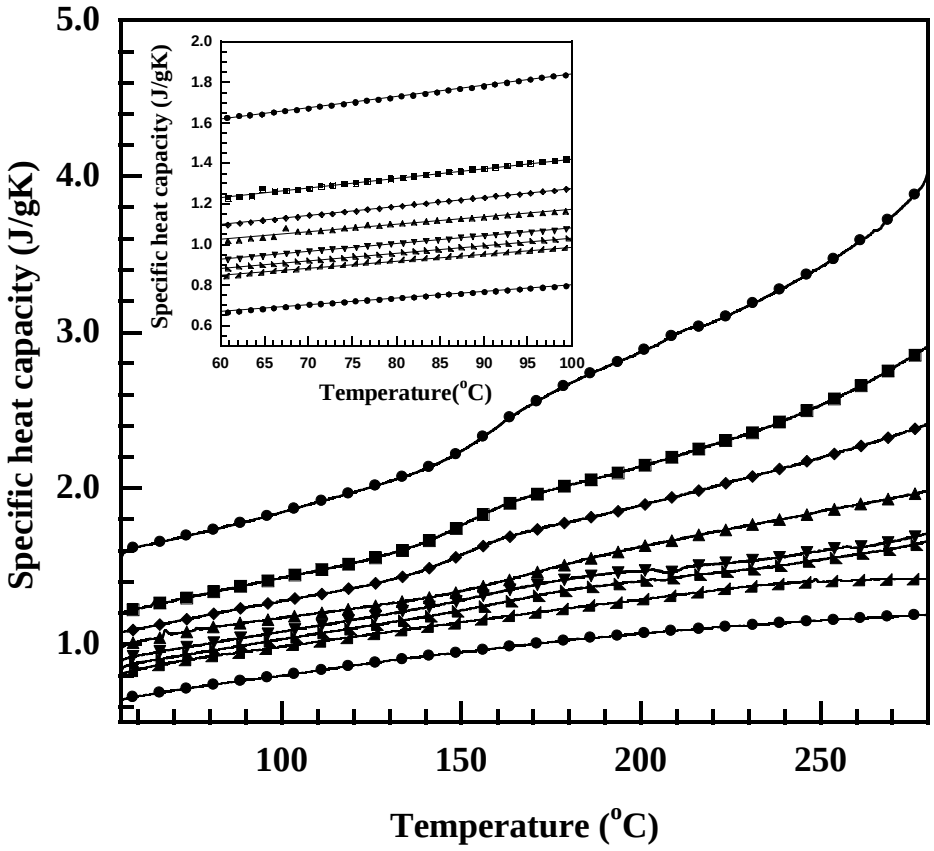

Figure 5.9 Specific heat capacity of graphite filled polybenzoxazine composites: (●) neat polybenzoxazine (■) 40wt%, (♦) 50wt%, (▲) 60wt%, (▼) 70wt%, (◣) 75wt%, (◢) 80wt%, (○) neat graphite

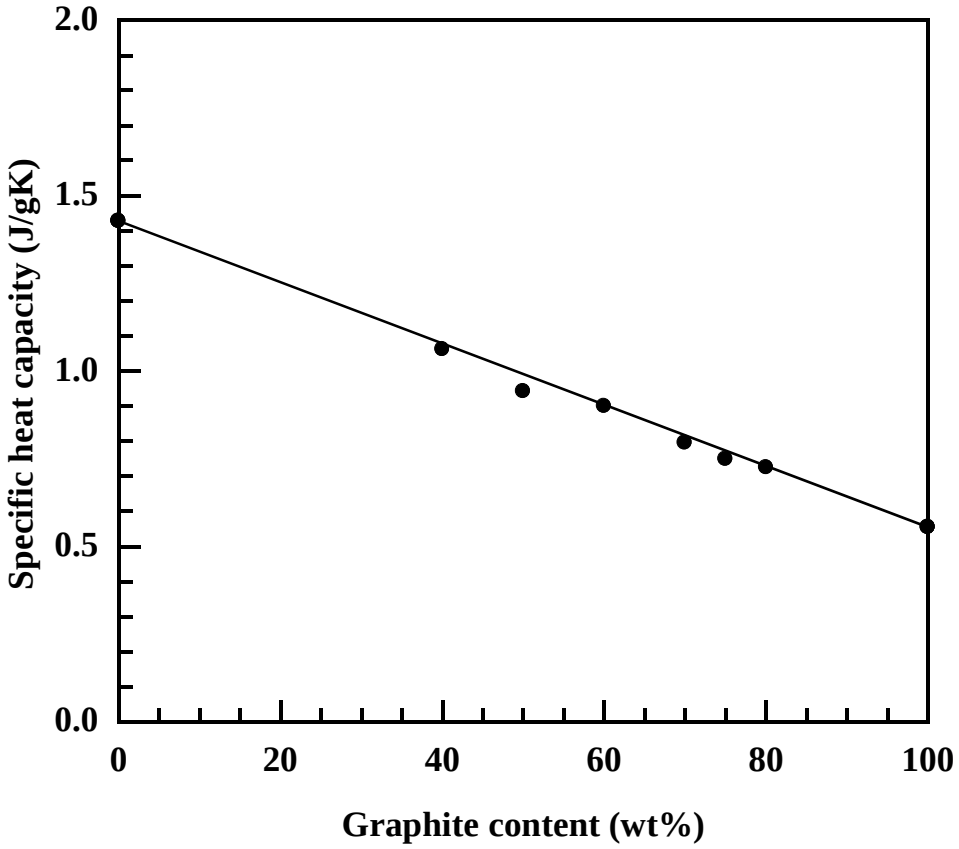

Figure 5.10 Thermal diffusivity at 25^{o}C of graphite filled polybenzoxazine as a function of filler contents.

Table 5.2 Heat capacity values of boron nitride-filled polybenzoxazine at different filler contents

Filler content wt%	Heat capacity $J\ K^{-1}\ kg^{-1}$		Error %
	Experimental	Calculated	
0	1.756	-	-
40	1.353	1.355	-0.13
50	1.212	1.255	-3.51
60	1.122	1.154	-2.87
70	1.025	1.054	-2.82
75	0.976	1.004	-2.84
80	0.937	0.954	-1.77
100	0.753	-	-

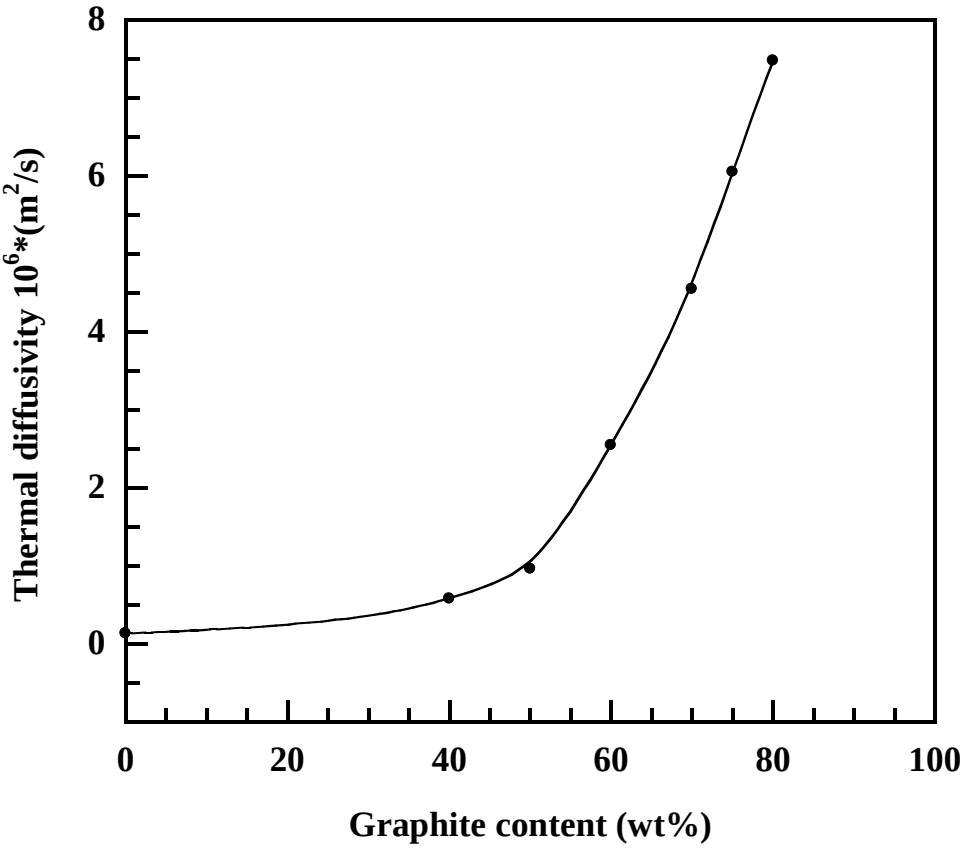

Figure 5.11 Thermal diffusivity at 25°C of graphite filled polybenzoxazine as a function of filler contents.

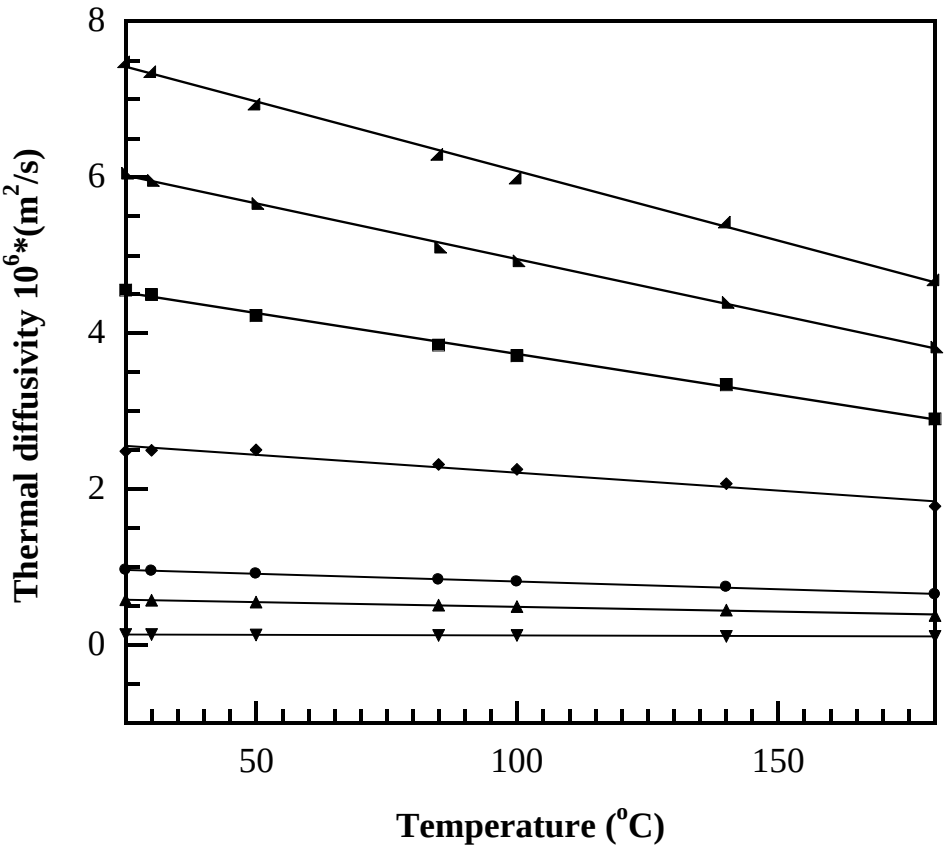

Figure 5.12 Thermal diffusivity of graphite filled polybenzoxazine composites: (●) neat polybenzoxazine (■) 40wt%, (♦) 50wt%, (▲) 60wt%, (▼) 70wt%, (◣) 75wt%, (◢) 80wt%

Table 5.3 Thermal conductivity of graphite-filled polybenzoxazine

Filler content	$\alpha \times 10^6$ (m^2/s)	C_p (J/kg K)	ρ (g/m^3)	k (W/mK)
0	0.133	1.427	1.200	0.228
40	0.577	1.063	1.452	0.890
50	0.963	0.942	1.537	1.394
60	2.546	0.900	1.635	3.744
70	4.550	0.795	1.746	6.314
75	6.051	0.749	1.806	8.185
80	7.482	0.725	1.877	10.185

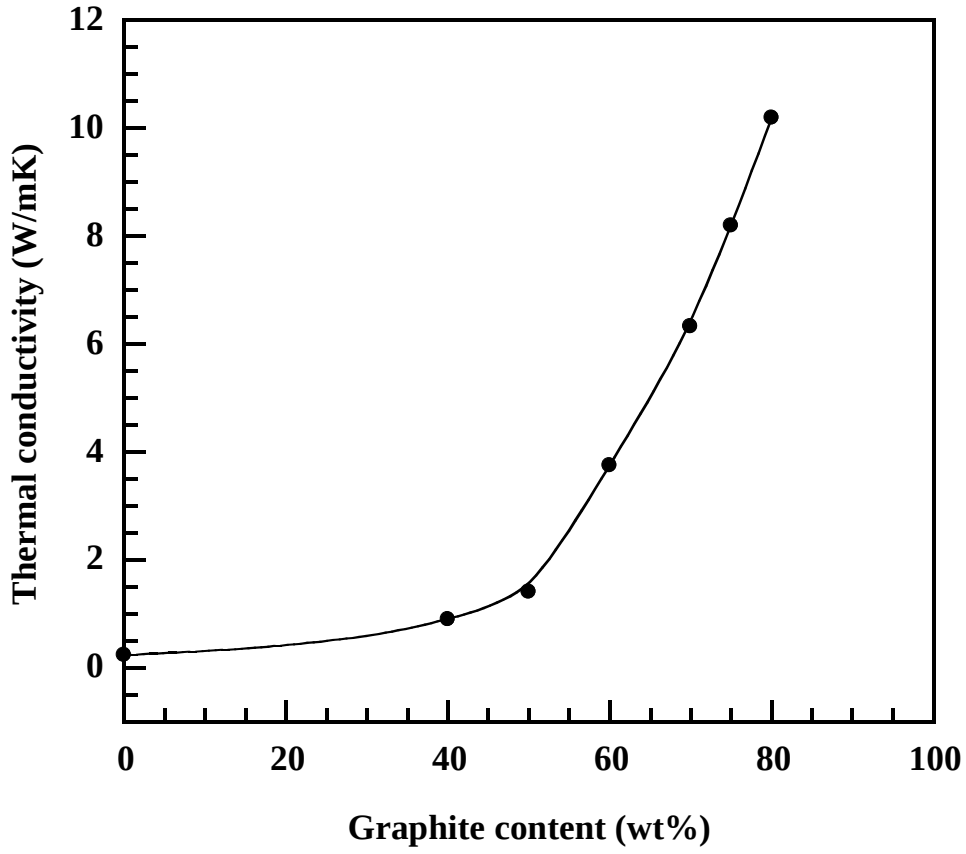

Figure 5.13 Thermal conductivity at 25^{o}C of graphite filled polybenzoxazine as a function of filler contents.

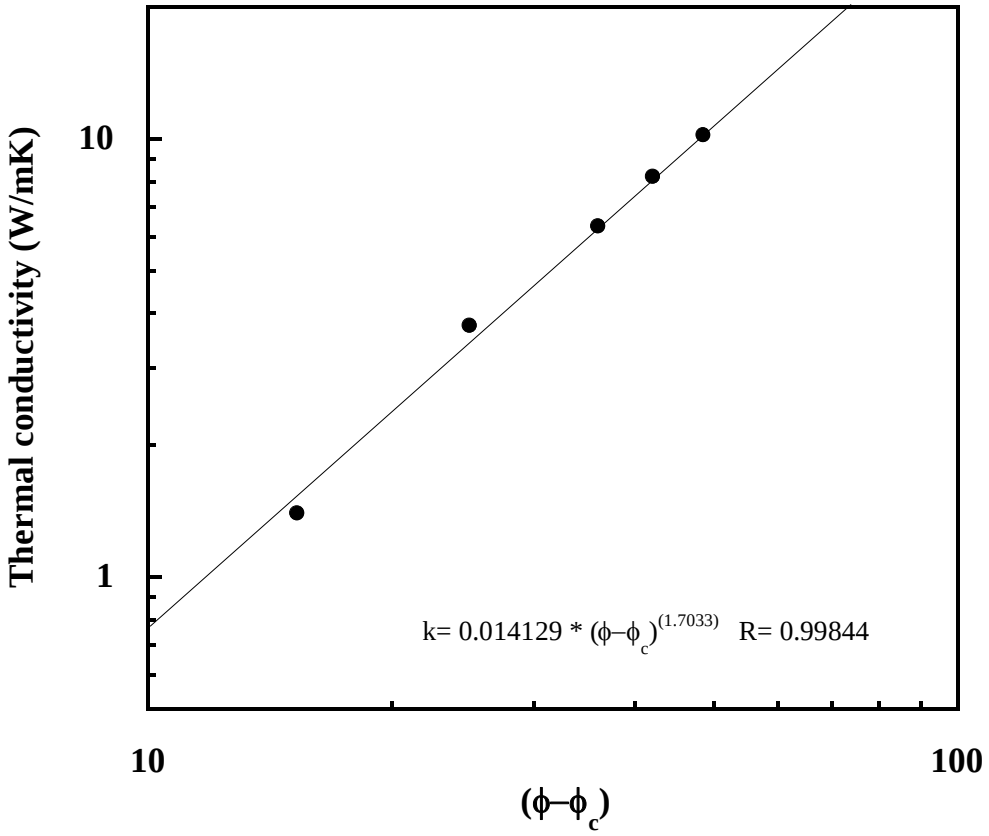

Figure 5.14 Percolation theory of thermal conductivity of graphite filled polybenzoxazine.

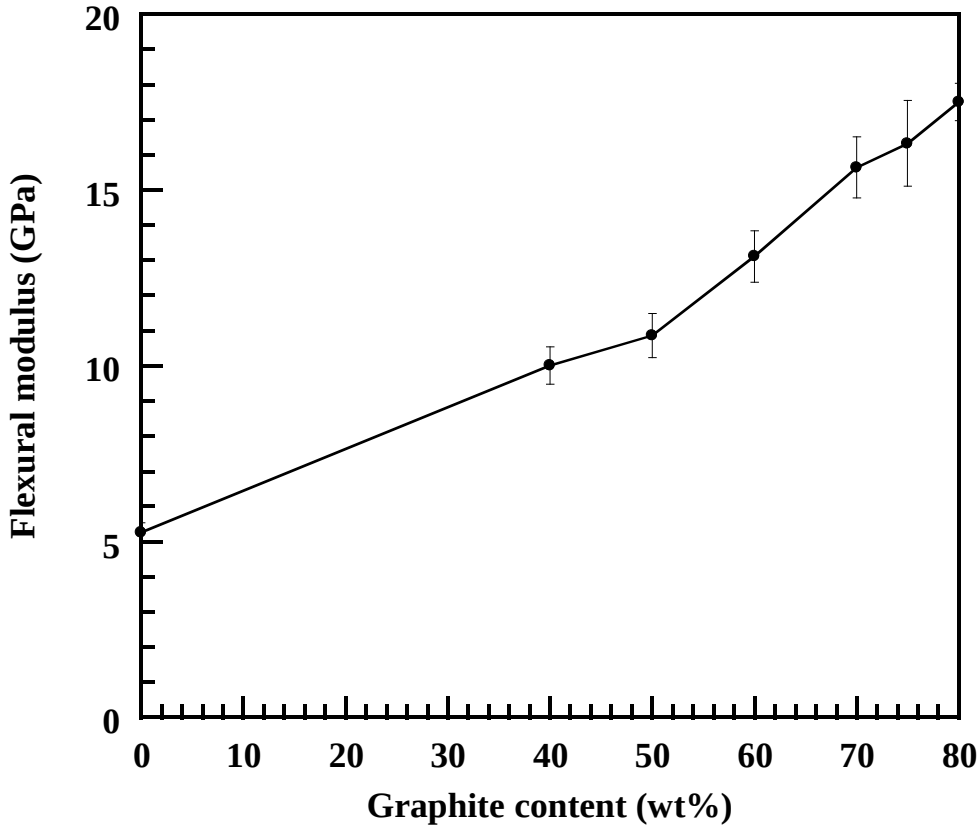

Figure 5.15 Relation between graphite content and the flexural modulus of graphite filled polybenzoxazine composites.

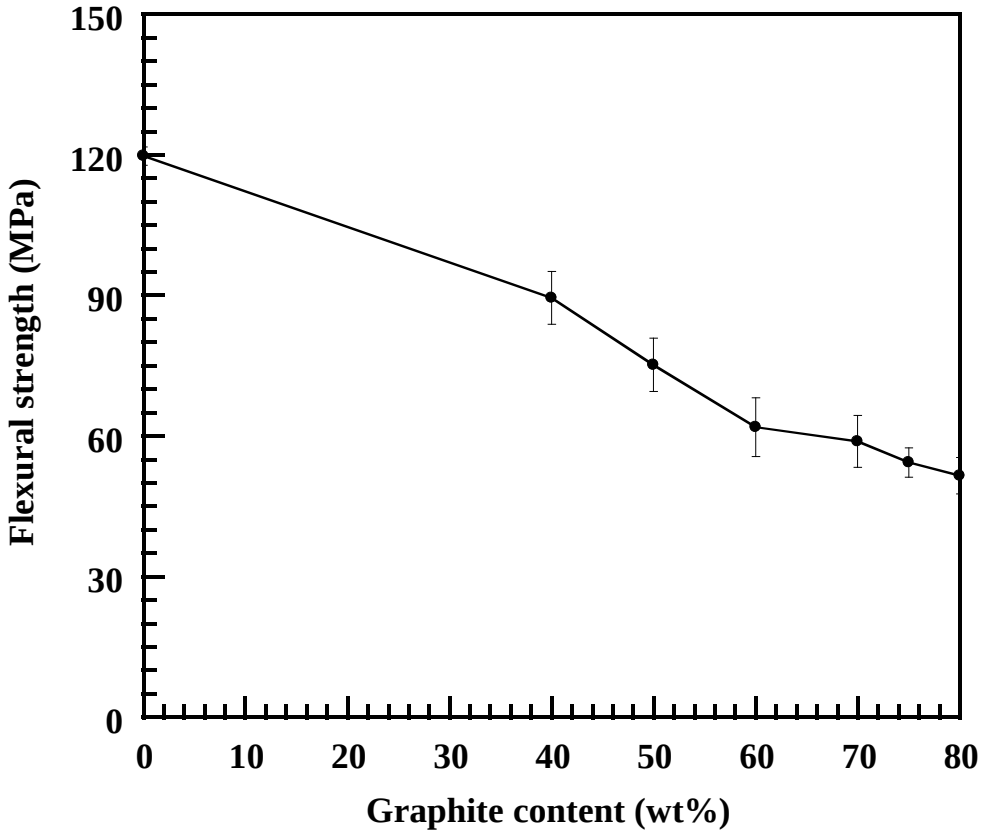

Figure 5.16 Relation between graphite content and the flexural strength of graphite filled polybenzoxazine composites.

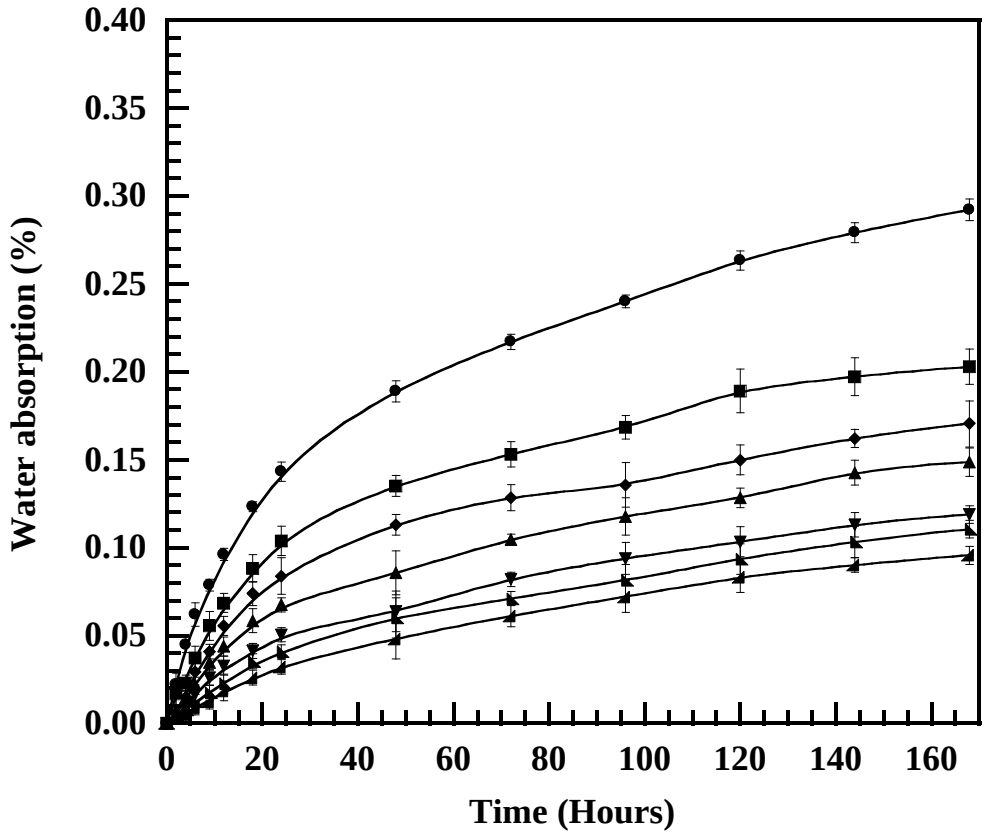

Figure 5.17 Water absorption of graphite filled polybenzoxazine composites: (●) neat polybenzoxazine (■) 40wt%, (♦) 50wt%, (▲) 60wt%, (▼) 70wt%, (◣) 75wt%, (◢) 80wt%.

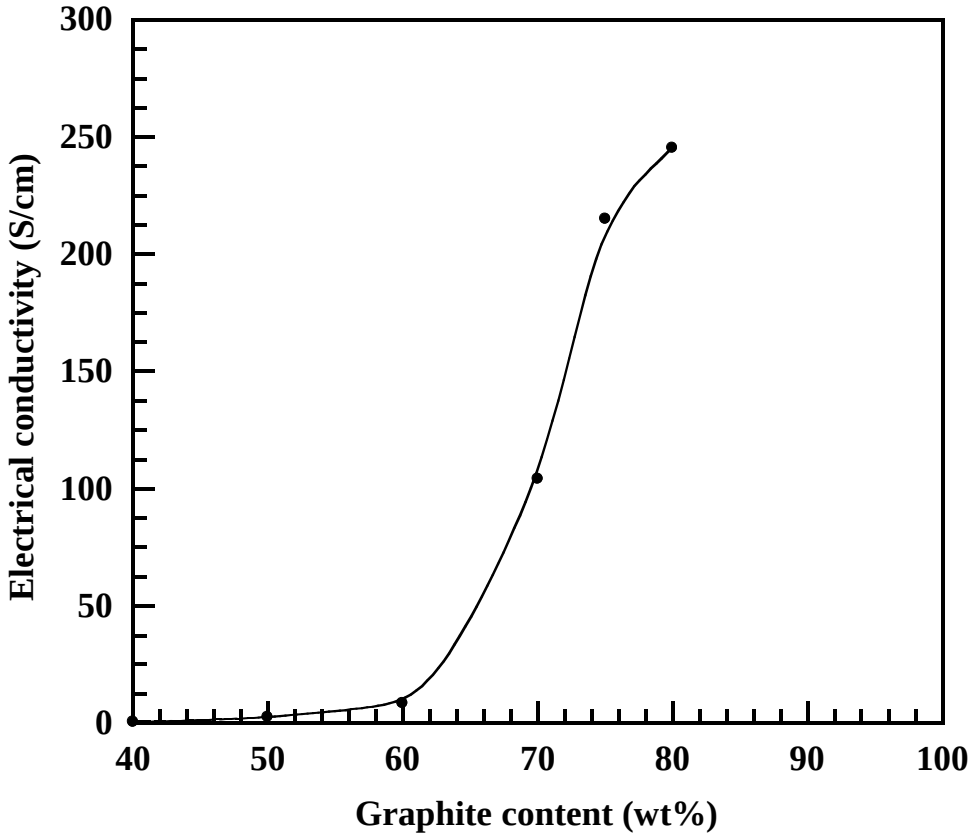

Figure 5.18 Effect of the graphite content on electrical conductivity (in-plane) of graphite filled polybenzoxazine composites.

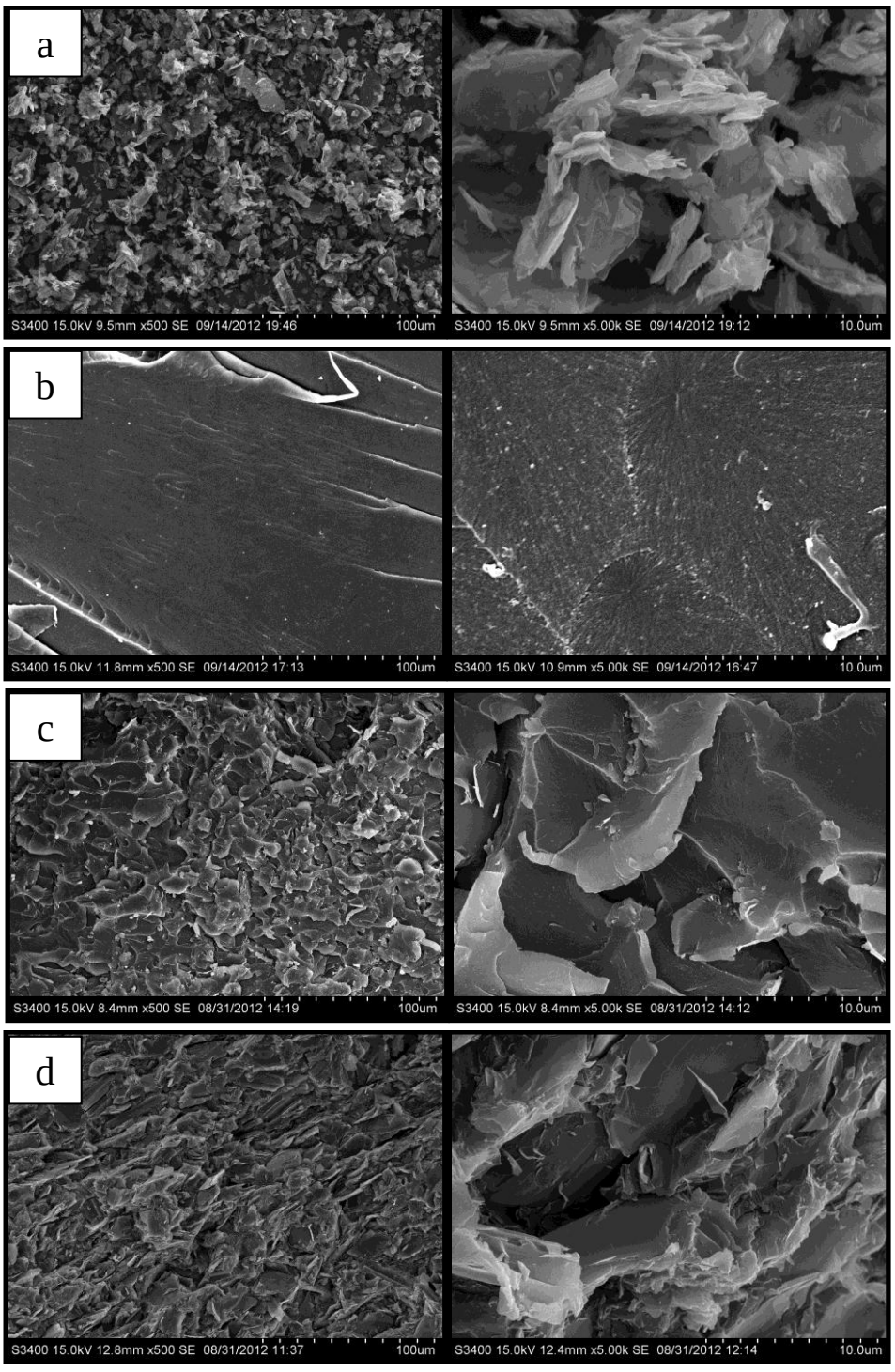

Figure 5.19 SEM micrographs of fracture surface of graphite-filled polybenzoxazine composites: (a) pure graphite, (b) neat polybenzoxazine (PBZ), (c) 5wt% graphite-filled PBZ, (d) 80wt% graphite-filled PBZ

CHAPTER VI

CONCLUSIONS

Highly filled systems of graphite and polybenzoxazine with the maximum graphite content of 80% were achieved in this work. The composites exhibit various properties highly suitable for a bipolar plate application comparing with most existing system and pass those requirements by the United States Department of Energy (DOE).

The DSC experiment revealed that the optimal curing condition to obtain the fully-cured specimens of the graphite-filled polybenzoxazine composites was by heating at 200^{o}C for 3 hours in a hydraulic hot-pressed machine at 15 MPa. The mechanical and thermal properties of graphite-filled polybenzoxazine composites at different graphite contents in the range 0 to 80 wt% tended to increase with increasing graphite contents. The actual density of the composites was measured to be close to the theoretical one suggesting negligible amount of void was presented in the composites. The glass transition temperature of graphite filled polybenzoxazine was found to increase with increasing the graphite contents, due to the substantial bonding between the polymer and the filler. The degradation temperatures (at 5% weight loss under nitrogen atmosphere) and solid residue (at 800^{o}C) of the composites were also observed to substantially increase with increasing the graphite contents.

In addition modulus of the highly filled polybenzoxazine composites was significantly improved by the presence of the graphite even at only few percent of the filler. Furthermore, the flexural strength slightly decreased whereas water absorption of the composites was significantly suppressed by the addition of the graphite-filler. Additionally, the storage modulus of the composite also exhibited the similar trend with the flexural modulus.

Finally, thermal conductivity and electrical conductivity of the composites were observed found to increase with increasing the graphite contents in a non-linear manner and can be predicted by bond percolation. Scanning electron micrographs revealed good filler-matrix interfacial adhesion with tight interfaces between the graphite and the polybenzoxazine matrix. The obtained mechanical properties, thermal properties and electrical conductivity of the highly filled graphite: polybenzoxazine composites are found to be highly attractive for bipolar plates in polymer electrolyte fuel cells (PEMFCs) application. Those properties were found to exceed those requirements set by DOE.

REFERENCES

[1] Bar-On, I., Kirchain, R. and Roth, R. Technical cost analysis of PEM fuel cells. J. Power Sources 109 (2002): 71-75.

[2] Liao, S.H., Yen, C.Y., Weng, C.C., Lin, Y.F., Ma, C.C.M., Yang, C.H., Tsai, M.C., Yen, M.Y., Hsiao, M.C., Lee, S.J., Xie, X.F. and Hsiao, Y.F. Preparation and properties of carbon nanotube/polypropylene nanocomposite bipolar plates for polymer electrolyte membrane fuel cells. J. Power Sources 185 (2008): 1225-1232.

[3] Guo, N. and Leu, M.C. Effect of different graphite materials on the electrical conductivity and flexural strength of bipolar plates fabricated using selective laser sintering. Int. J. Hydrogen Energy 37 (2012): 3558-3566.

[4] Vielstich, W., Gasteiger, H.A. and Lamm, A. Handbook of fuel cells-fundamentals technology and applications, 3th edition, Wiley & Sons, New York. (2003).

[5] Ning, X. and Ishida, H. Phenolic materials via ring-opening polymerization of benzoxazines: effect of molecular structure on mechanical and dynamic mechanical properties. J. Polym. Sci., Part B 32 (1994): 921-927.

[6] Wang, Y.X. and Ishida, H. Development of low-viscosity benzoxazine resins and their polymers. J. Appl. Polym. Sci. 86 (2002): 2953-2966.

[7] Rimdusit, S., Tanthapanichakoon, W. and Jubsil, C. High performance wood composites from highly filled polybenzoxazine. J. Appl. Polym. Sci. 99 (2006): 1240-1253.

[8] Ishida, H. and Rimdusit, S. Very high thermal conductivity obtained by boron nitride-filled polybenzoxazine. Thermochimica Acta 320 (1998): 177-186.

[9] Weaver, G., World fuel cells-an industry profile with market prospects to 2010. New York: Elsevier 1 (2010): 234.

[10] Sopian, K. and Daud, W.R.W. Challenges and future developments in proton exchange membrane fuel cells. Renewable Energy 31 (2006): 719-727.

[11] Barbir, F. PEM Fuel Cell. UK: Elsevier Inc. (2005).

[12] Larmininie, J. and Dicks, A. Fuel Cell Systems Explained. West Sussex, England: John Wiley and Sons Ltd. 2 (2003).

[13] Vishnyakov, V.M. Proton exchange membrane fuel cells. J. Vac. Sci. Technol., A 80 (2006): 1053-1065.

[14] Kusie, J., Knight, J. and Morton, J. News Release. 2010, Ministry of Transportation and Infrastructure BC, Canada.

[15] Hayre, R., Cha, S.W., Colella, W. and Prinz, F.B. Fuel cell fundamentals, ed. 2nd. 2009, New York: Jonhn Wiley and Sons, Inc.

[16] Mehta, V. and Cooper, J.S. Review and analysis of PEM fuel cell design and manufacturing. J. Power Sources 114 (2003): 32-53.

[17] Cooper, J.S. Design Analysis of PEMFC Bipolar Plates Considering Stack Manufacturing and Environment Impact. J. Power Sources 129 (2004): 152-169.

[18] Besmann, T.M., Klett, J. W., Henry, J. J. and Lara, C.E. Carbon/Carbon Composite Bipolar Plate for PEM Fuel Cells. J. Electrochem. Soc. 147 (2000): 4083-4086.

[19] Jayakumar, K., Pandiyan, S., Rajalakshmi,N. and Dhathathreyan, K.S. Cost-benefit analysis of commercial bipolar plates for PEMFC's. J. Power Sources 161 (2006): 454–459.

[20] On, I.B., Kirchain, R. and Roth, R. Technical cost analysis for PEM fuel cells. J. Power Sources 109 (2002): 71-75.

[21] Dihrab, S.S., Sopian, K., Alghoul, M.A. and Sulaiman, M.Y. Review of The membrane and bipolar plates materials for conventional and unitized regenerative fuel cells. Renewable and Sustainable Energy Reviews 13 (2009): 1663–1668.

[22] Xiao, M., Lub, Y., Wang, S.J., Zhaoa, Y.F. and Menga, Y.Z. Poly(arylene disulfide)/graphite nanosheets composites as bipolar plates for polymer electrolyte membrane fuel cells. J. Power Sources 160 (2006): 165-174.

[23] Du, C., Ming, P., Hou, M., Fu, J., Shen, Q., Liang, D., Fu, Y., Luo, X., Shao, Z., Yi, B. Preparation and properties of thin epoxy/compressed expanded graphite composite bipolar plates for proton exchange membrane fuel cells. J. Power Sources 195 (2010): 794–800.

[24] Heo, S.I., Oh, K.S., Yun, J.C., Jung, S.H., Yang, Y.C. and Han, K.S. Development of preform moulding technique using expanded graphite for proton exchange membrane fuel cell bipolar plates. J. Power Sources 171 (2007): 396–403.

[25] Tawfika, H., Hunga, Y. and Mahajan, D. Metal bipolar plates for PEM fuel cell-a review. J. Power Sources 163 (2007): 755-767.

[26] Antunes, R.A., Oliveira, M.C.L., Ett, G. and Ett, V. Corrosion of metal bipolar plates for pem fuel cells: a review. Int. J. Hydrogen Energy 35 (2010): 3632-3647.

[27] Hung, Y., Khatib, K.M. and Tawfik, H. Corrosion-resistant lightweight metallic bipolar plates for PEM fuel fells. J. Appl. Electrochem. 35 (2005): 445-447.

[28] Wind, J. Metallic bipolar plates for PEM fuel cells. J. Power Sources 105 (2002): 256-260.

[29] Davies, D.P., Spah, R., Kaiser, W. and Bohm, G. Bipolar plate materials for solid polymer fuel cells. J. Appl. Electrochem. 30 (2000): 101-105.

[30] Enin, A., Salam, S.A. and Omar, E. New electroplated aluminum bipolar plate for PEM fuel cell. J. Power Sources 177 (2008): 131–136.

[31] Davies, D.P., Adcock, P.L., Turpin, M. and Rowen, S.J. Stainless steel as a bipolar plate material for solid polymer fuel cells. J. Power Sources, 86 (2000): 237-242.

[32] Wang, H., Sweikart, M.A. and Turner, J.A. Stainless steel as bipolar plate material for polymer electrolyte membrane fuel cells. J. Power Sources 115 (2003): 249-251.

[33] Joseph, S., McClure, J.C., Chianelli, R., Pich, P. and Sebastian, P.J. Conducting polymer-coated stainless steel bipolar plates for proton exchange membrane fuel cells (PEMFC). Int. J. Hydrogen Energy 30 (2005): 1339-1344.

[34] Cunningham, N., Dodeleta, J.P., Guaya, D. and Ross, G.G. RBS and XRD Analyses of carbon-coated stainless steel plates. Surf. Coat. Technol. 183 (2004.): 216-223.

[35] Ku, C.C. and Liepins, R. Electrical properties of polymers: chemical principles. New York: Hanser Publishing (1987).

[36] Donald, W.O. GRAPHITE, U.S. geological survey minerals yearbook 33 (2003): 1-10.

[37] Hehr, B.D. High temperature graphite simulations using molecular dynamics, A thesis submitted to the graduate faculty of North Carolina State University (2007): 5-7.

[38] Ferro-Ceramic Grinding Inc. (2007). Graphite (Online). Available: http://www.ferroceramic.com/graphite_table.htm [2011,may 10]

[39] Webb, T.C. and Stewart, H.J. Graphite new brunswick department of natural resources; minerals, policy and planning division, mineral commodity profile. 3 (2009): 1-6.

[40] Ishida, H. Process of benzoxazine compounds in solventless systems. U.S. Patent 5,543,516 (1996).

[41] Ishida, H. and Allen, D. J., Mechanical characterization of copolymers based on benzoxazine and epoxy. J. Polymer 37 (1996): 4487-4495.

[42] Rimdusit, S., Pirstpindvong, S., Tanthapanichakoon, W. and Damrongsakkul, S. Toughening of polybenzoxazine by alloying with urethane prepolymer and flexible epoxy: a comparative study. J. Polym. Eng. and Sci. 45 (2005): 228.

[43] Lide, D.R. Handbook of Chemistry and Physics 85th edition, CRC Press, New York (2004).

[44] Ishida, H. and Sanders, D.P. Improved thermal and mechanical properties of polybenzoxazines based on alkyl-substituted aromatic amines. J. Polym. Sci. Part B, Polym. Phys. 38 (2000): 3289-3301.

[45] Kuan, H. C., Ma, C. C. M. and Chen S. M. Preparation, electrical, mechanical and thermal properties of composite bipolar plate for a fuel cell. J. Power Sources 134 (2004): 7-17.

[46] Priyanka, H., Maheshwari, R.B. and Mathur, T.L. Fabrication of high strength and a low weight composite bipolar plate for fuel cell applications. J. Power Sources 173 (2007): 394–403.

[47] Kang, S. J., et al. Solvent-assisted graphite loading for highly conductive phenolic resin bipolar plates for proton exchange membrane fuel cells. J. Power Sources 195 (2010): 3794–3801.

[48] Chen H., Liu H. and He Y. Effects of resin type on properties of graphite/polymer composite bipolar plate for proton exchange membrane fuel cell. J. Mater. Res. 26 (2011): 2974-2979.

[49] Chen W., Liu Y. and Xin Q. Evaluation of a compression molded composite bipolar plate for direct methanol fuel cell. Int. J. Hydrogen Energy 35 (2010): 3783-3788.

[50] Kim, J. W., et al. Synergy effects of hybrid carbon system on properties of composite bipolar plates for fuel cells. J. Power Sources 195 (2010): 5474–5480.

[51] Ishida, H. and Rimdusit, S. Heat capacity measurement of boron nitride-filled polybenzoxazine. J. Therm. Anal. Calorim. 58 (1999): 497-507.

[52] Xu, Y., Ray, G. and Magid, B. A. Thermal behavior of single-walled carbon nanotube polymer-matrix composites. Composites Part A 37 (2006): 114–121.

[53] Kimura, H., Ohtsuka, K. and Matsumoto, A. Performance of graphite filled composite based on benzoxazine resin. J. Appl. Polymer. Sci. 117 (2010): 1711-1717.

[54] Rimdusit, S. and Ishida, H. Development of new class of electronic packaging materials based on ternary systems of benzoxazine, epoxy, and phenolics resins. Polymer 41(2000): 7941.

[55] Kasemsiri, P., Hiziroglu, S. and Rimdusit, S. Effect of cashew nut shell liquid on gelation, cure kinetics, and thermomechanical properties of benzoxazine resin. Thermochim. Acta. 520 (2011): 84-92

[56] Rao, B.S. and Palanisamy, A. Monofunctional benzoxazine from cardanol for bio-composite applications. React. Funct. Polym. 71 (2011): 148-154

[57] Jubsilp, C., Takeichi, T. and Rimdusit, S. Polymerization kinetics. Handbook of benzoxazine resins Chapter 7 (2011): 157-174

[58] Kuan, H. C., Ma, C. C. M. and Chen S. M. Preparation, electrical, mechanical and thermal properties of composite bipolar plate for a fuel cell. J. Power Sources 134 (2004): 7-17.

[59] Kim, J.W., Kim, N.H., Kuilla, T., Kim, T.J., Rhee, K.Y. and Lee, J.H. Synergy effects of hybrid carbon system on properties of composite bipolar plates for fuel cells. J. Power Sources 195 (2010): 5474-5480.

[60] Du, L. and Jana, S.C. Highly conductive epoxy/graphite composites for bipolar plates in proton exchange membrane fuel cells. J. Power Sources 172 (2007): 734-741.

[61] Otieno, G. and Kim, J.Y. Conductive graphite/polyurethane composite films using amphiphilic reactive dispersant: synthesis and characterization. J. Ind. Eng. Chem. 14 (2008): 187–193.

[62] Liu, D., Purewal, J.J., Yang, J., Sudik, A., Maurer, S., Mueller, U., Ni, J. and Siegel, D.J. MOF-5 composites exhibiting improved thermal conductivity. Int. J. Hydrogen Energy 37 (2012) 6109-6117.

[63] Haoming, T. and Lin, Y.. Thermal conductive PS/graphite composites. Polym. Adv. Technol. 20 (2009) 21-27.

[64] Agoudjil, B., Ibos, L., Majeste, J.C., Candau, Y. and Mamunya, Y.P. Correlation between transport properties of ethylene vinyl acetate/glass, silver-coated glass spheres composites. Composites Part A 20 (2009) 21-27.

[65] Min, C.H., Shu, H.L., Ming, Y.Y., Chen, C.M., Shuo, J.L., Yung, H.C., Chih H.H. Yu F.L. and Xiao, F.X. Electrical and thermal conductivities of novel metal mesh hybrid polymer composite bipolar plates for proton exchange membrane fuel cells. J. Power Sources 195 (2010) 509-515.

[66] Hwang, I.U., Yu, H.N., Kim, S.S., Lee, D.G., Suh, J.D., Lee, S.H., Ahn, B.K., Kim, S.H. and Lim, T.W. Bipolar plate made of carbon fiber epoxy composite for polymer electrolytemembrane fuel cells. J. Power Sources 184 (2008): 90-94.

[67] Maheshwari, P.H., Mathur, R.B. and Dhami, T.L. Fabrication of high strength

and a low weight composite bipolar plate for fuel cell applications. J. Power Sources 173 (2007): 394-403.

[68] Kim, J.W., Kim, N.H., Kuilla, T., Kim, T.J., Rhee, K.Y. and Lee, J.H. Synergy effects of hybrid carbon system on properties of composite bipolar plates for fuel cells. J. Power Sources 195 (2010): 5474-5480.

[69] Kang, S.J., Kim, D.O., Lee, J.H., Lee, P.C., Lee, M.H., Lee, Y., Lee, J.Y., Choi, H.R., Lee, J.H., Oh, Y.S. and Nam, J.D. Synergy effects of hybrid carbon system on properties of composite bipolar plates for fuel cells. J. Power Sources 195 (2010): 5474-5480.

[70] Hui, C., Hong, L., Li, Y. and Yue, H. Effects of resin type on properties of graphite/polymer composite bipolar plate for proton exchange membrane fuel cell. J. Mater. Res. 26 (2011): 2974-2979.

[71] Du, L. and Jana, S.C. Hygrothermal effects on properties of highly conductive epoxy/graphite composites for applications as bipolar plates. J. Power Sources 182 (2008): 223–229.

[72] Cho, E.A., Jeon, U.S., Ha, H.Y., Hong, S.A., Oh, I.H. Characteristics of composite bipolar plates for polymer electrolyte membrane fuel cells. J. Power Sources 125 (2004): 178-182.

[73] Du, L. and Jana, S.C. Highly conductive epoxy/graphite composites for bipolar plates in proton exchange membrane fuel cells. J. Power Sources 172 (2007): 734-741.

[74] Kim, J.W., Kim, N.H., Kuilla, T., Kim, T.J. Rhee, K.Y. and Lee, J.H. Synergy effects of hybrid carbon system on properties of composite bipolar plates for fuel cells. J. Power Sources 195 (2010): 5474-5480.

[75] Chen, W., Liu, Y. and Xin, Q. Evaluation of a compression molded composite bipolar plate for direct methanol fuel cell. Int. J. Hydrogen Energy 35 (2010): 3783-3788.

[76] Dhakate, S.R., Sharma, S., Borah, M., Mathur, R.B. and Dhami, T.L. Expanded graphite-based electrically conductive composites as bipolar plate for PEM fuel cell. Int. J. Hydrogen Energy 33 (2008): 7146-7152.

APPENDICES

APPENDIX A

Characterization of Graphite filled Polybenzoxazine Composites

Appendix A-1 The maximum packing density of graphite filled benzoxazine resin composites.

Graphite content (wt%)	Graphite content (vol%)	Theoretical density (g/cm3)	Actual density (g/cm3)
0	0	1.1900	1.2000
40	26.5	1.4577	1.4520
50	35.1	1.5445	1.5370
60	44.8	1.6424	1.6350
70	55.8	1.7535	1.7460
75	61.9	1.8149	1.8060
80	68.5	1.8807	1.8767

Appendix A-2 The storage modulus (E') at 35^{o}C and the glass transition temperature (Tg, loss modulus), of graphite filled polybezoxazine composites at various graphite contents which were determined from DMA.

Graphite content (wt%)	Storage modulus (E') at 35^{o}C (MPa)	Glass transition temperature (^{o}C)
0	5950	176
40	10717	185
50	12696	189
60	15889	191
70	17794	192
75	19245	194
80	23029	195

Appendix A-3 Mechanical properties of graphite filled polybenzoxazine composite at room temperature.

Graphite content (wt%)	Flexural modulus (GPa)	Flexural strength (MPa)
0	5.2520 ± 0.276	119.70 ± 1.929
40	9.9990 ± 0.530	89.423 ± 5.618
50	10.856 ± 0.629	75.137 ± 5.691
60	13.104 ± 0.733	61.913 ± 6.275
70	15.635 ± 0.872	58.797 ± 5.559
75	16.316 ± 1.217	54.310 ± 3.117
80	17.497 ± 0.524	51.520 ± 3.864

Appendix A-4 Water absorption of graphite filled polybenzoxazine composites at various graphite contents.

Graphite content (wt%)	24 hr (%)	7days (%)
0	0.143 ± 0.005	0.292 ± 0.006
40	0.104 ± 0.008	0.203 ± 0.010
50	0.084 ± 0.010	0.170 ± 0.013
60	0.067 ± 0.004	0.149 ± 0.008
70	0.050 ± 0.004	0.119 ± 0.005
75	0.040 ± 0.004	0.110 ± 0.005
80	0.032 ± 0.004	0.095 ± 0.005

VITA

Mr. Anucha Pengdam was born in Nakornsrithammarat, Thailand. He graduated at high school level in 2007 from Prasangwittaya School. He received the Bachelor's Degree of Science with a major in Chemistry from the Faculty of Engineer, Prince of Songkla University, Thailand in 2010. After graduation, he entered study for a Master's Degree of Chemical Engineering at the Department of Chemical Engineering, Faculty of Engineering, Chulalongkorn University.

Some part of this work was selected for poster presentation in The Seventh International Conference on Materials Science and Technology which was held during June 7-8, 2012 at Swissotel Le Concerde, Bangkok, Thailand